

CHAPTER 1

DENSITY FUNCTIONAL THEORY

George F. Bertsch

*Institute for Nuclear Theory
and Department of Physics and Astronomy
University of Washington Seattle WA 98195 USA
E-mail: bertsch@u.washington.edu*

Kazuhiro Yabana

*Institute of Physics
University of Tsukuba
Tsukuba 305-8577 Japan*

Density functional theory is a remarkably successful theory of ordinary matter, despite its *ad hoc* origins. These lectures describe the theory and its applications starting from an elementary level. The practical theory uses the Kohn-Sham equations, well-chosen energy functionals, and efficient numerical methods for solving the Schroedinger equation. The time-dependent version of the theory is also useful for describing excitations. These notes are based on courses given by one of the authors (GFB) at the Graduiertenkolleg in Rostock, Germany in March 2001 and the Summer School on Microscopic Quantum Many-Body Theories in Trieste, Italy in September 2001.

1. Introduction

The density functional theory is now widely applied in all areas of physics and chemistry, wherever properties of systems of electrons need to be calculated. The theory is very successful in calculating certain properties—hence its popularity. This is reason enough for a student of theory to learn what it is all about. However, it is quite different in philosophy to other many-body approaches that you will hear about. The tried-and-true path in theoretical physics is to look for systematic expansions for calculating the properties of interest, finding controlled approximations that be refined to achieve greater accuracy. The density functional theory is not at all systematic, and in the end its justification is only the quality of its predictions. However, it is rightly described as an *ab initio* framework, giving theories whose parameters are determined *a priori* by general considerations. These lectures will present the theory and its applications at a pace that I hope is understandable with a minimum of prior formal training in advanced quantum mechanics. In the first

lecture today, I will set the stage by deriving Hartree-Fock theory, presenting some results on the homogeneous electron gas, and finally presenting the Hohenberg-Kohn theorem, which has motivated the density functional approach.

I will begin the next lecture with a simple example of a density functional theory which can be worked out, ending up with the Thomas-Fermi theory of many-electron systems. Unfortunately, the Thomas-Fermi theory has very limited validity, and it has not been possible to make useful improvements despite many attempts. The DFT became useful only after Kohn and Sham introduced electron orbitals into the functional. In their theory the variables are the single-particle wave functions of electrons in occupied orbitals as well as the electron density. The theory then has a structure very close to mean-field theories such as the Hartree theory. The emphasis on using the density variable wherever possible leads directly to a version of the theory called the Local Density Approximation (LDA). The LDA is a significant improvement over Hartree-Fock (in ways we shall discuss), but at the same time one can see deficiencies inherent in that scheme. A more complicated implementation of the theory, called the Generalized Gradient Approximation, makes it surprising accurate for calculating structures and binding energies, and in this form the theory is widely applied.

The Kohn-Sham theory requires solving the 3-dimensional Schroedinger equation many times, and questions of algorithms and numerical methods are important in making applications of the theory. There are several well-developed methods to solve the equations, and each has its advocates. In my third lecture I will discuss some of these numerical aspects. I will also survey some of the applications, noting where the DFT is reliable and where its accuracy is problematic. I will also mention some directions that have been taken to make more accurate theories, going beyond the DFT.

All of this so far is a theory of matter in its ground state. We are of course also very interested in the excitations of many-body systems, and the DFT can also be applied to dynamics, where it is called time-dependent density functional theory (TDDFT). In my fourth lecture I will derive the equations to be solved and the algorithms used to solve the equations. The time-dependent theory is quite computationally intensive, and much progress can be made by finding more efficient numerical techniques. Finally, in the last lecture, I will show you some state-of-the-art applications of the TDDFT.

Although it is not really necessary for my lectures, I will use a second-quantized field operator notation because it is the most efficient way to write down expectation values in many-particle spaces. Let us start with the basic Hamiltonian, which can be taken as the sum of three terms,

$$\begin{aligned}
 H = & \int d^3r \frac{\hbar^2}{2m} \nabla \psi^\dagger(\mathbf{r}) \cdot \nabla \psi(\mathbf{r}) + \frac{1}{2} \int d^3r \int d^3r' \frac{e^2}{|\mathbf{r} - \mathbf{r}'|} \psi^\dagger(\mathbf{r}) \psi^\dagger(\mathbf{r}') \psi(\mathbf{r}') \psi(\mathbf{r}) \\
 & + \int d^3r V_{ext}(\mathbf{r}) \psi^\dagger(\mathbf{r}) \psi(\mathbf{r}).
 \end{aligned} \tag{1.1}$$

The terms represent the electron kinetic energy, the electron-electron interaction, and the interaction of the electrons with an external field, respectively. The ψ^\dagger and ψ are field operators with the Fermion anticommutation relations, $\{\psi^\dagger(\mathbf{r}), \psi(\mathbf{r}')\} = \delta(\mathbf{r} - \mathbf{r}')$. I will explain what one needs to know about these as we go along. As a warm-up to the theory, I will derive the Hartree-Fock theory. But before that, some issues of notation and units should be clarified.

1.1. Units and notation

In eq. 1.1 we used units in which e^2 has dimensions of energy-length. If you are used to the MKS system, you can convert formulas by the substitution $e^2 \rightarrow e_{MKS}^2/4\pi\epsilon_0$. One often sees formulas quoted in atomic units, with no explicit dimensional quantities. In atomic units, lengths are expressed in units of the Bohr, $a_0 = \hbar^2/me^2 = 0.529.. \text{ \AA}$ and energies in units of the Hartree, $e^2/a_0 = 27.2. \text{ eV}$. Confusingly, one also sees energies quoted in Rydbergs, $e^2/2a_0 = 13.6.. \text{ eV}$. Personally, I do not care for implicit atomic units because they hide the functional dependence on mass and charge. It is also common to express densities in terms of the parameter r_s , defined as the radius in atomic units of a sphere whose volume is the reciprocal density. Thus $r_s = (3n/4\pi)^{1/3}\hbar^2/me^2$, where n is the density of electrons. In presenting numerical results, I will often use “practical atomic units”, taking eV for energy and \AA (0.1 nm) for length.

1.2. Hartree-Fock theory

Hartree-Fock theory is very simple to describe: it is the variational theory obtained by the expectation value of the Hamiltonian, allowing all wave functions that can be represented as Slater determinants. Let's see how this comes about. Using second-quantized notation, the Slater determinants constructed from a set of orthonormal single-particle wave functions $\{a\}$ are represented by a product of creation operators c^\dagger acting on the vacuum. An N -particle state is thus

$$|N\rangle = \sum_a^N c_a^\dagger | \rangle.$$

The operators c^\dagger and c satisfy the anticommutation relation $\{c_a^\dagger, c_{a'}\} = \delta_{a,a'}$. To get back the orbital wave function in position space, i.e. to reveal the spatial wave function $\phi_a(\mathbf{r})$, we apply the field operator $\psi(\mathbf{r})$ to the state a . The anticommutator gives the sought amplitude,

$$\{\psi(\mathbf{r}), c_a^\dagger\} = \phi_a(\mathbf{r}).$$

We now take the expectation value of H in the state $|N\rangle$ and reduce the operator expectation values by moving annihilation operators to the right and creation operators to the left with the help of the above anticommutators. The result at the

end is

$$\begin{aligned} \langle N|H|N\rangle &= \sum_a^N \frac{\hbar^2}{2m} \int d^3r \nabla \phi_a^* \cdot \nabla \phi_a + \sum_{a<b} \int d^3r \int d^3r' \frac{e^2}{|\mathbf{r}-\mathbf{r}'|} |\phi_a|^2 |\phi_b|^2 \\ &- \sum_{a<b} \int d^3r \int d^3r' \frac{e^2}{|\mathbf{r}-\mathbf{r}'|} \phi_a^*(\mathbf{r}) \phi_a(\mathbf{r}') \phi_b^*(\mathbf{r}') \phi_b(\mathbf{r}) + \sum_a \int d^3r V_{ext}(\mathbf{r}) |\phi_a|^2. \end{aligned} \quad (1.2)$$

The result looks very similar to eq. (1.1) with respect to the kinetic energy and the external potential energy terms. But the electron-electron interaction has given rise to two terms, the direct (or Hartree) energy, and the exchange (or Fock) energy. Notice also that the factor of 1/2 in eq. (1.1) has disappeared; instead one has a double sum over the $N(N-1)/2$ orbital pairs (a, b) . It is often convenient to rewrite eq. (1.2) rearranging the sums slightly. Let us add terms with $a = b$ to the direct and exchange sums. This won't affect the result, because the direct and exchange cancel if the two orbitals are the same. The direct term can then be written as an independent sum over the a and b orbitals. Defining the single particle density $n(\mathbf{r}) = \langle N|\psi^\dagger(\mathbf{r})\psi(\mathbf{r})|N\rangle = \sum_a^N |\phi_a(\mathbf{r})|^2$, the direct and external field terms are seen to depend directly on $n(\mathbf{r})$. The full expectation value becomes

$$\begin{aligned} \langle N|H|N\rangle &= \sum_a^N \frac{\hbar^2}{2m} \int d^3r \nabla \phi_a^* \cdot \nabla \phi_a + \frac{1}{2} \int d^3r \int d^3r' \frac{e^2}{|\mathbf{r}-\mathbf{r}'|} n(\mathbf{r})n(\mathbf{r}') \\ &- \sum_{a<b} \int d^3r \int d^3r' \frac{e^2}{|\mathbf{r}-\mathbf{r}'|} \phi_a^*(\mathbf{r}) \phi_a(\mathbf{r}') \phi_b^*(\mathbf{r}') \phi_b(\mathbf{r}) \\ &+ \int d^3r V_{ext}(\mathbf{r})n(\mathbf{r}). \end{aligned} \quad (1.3)$$

Now that we have the Hartree-Fock energy function, the next task is to find the minimum within the allowed variational space. First let us recall quickly how variational principles work. If we have an integral expression $\int F(\phi)dx$ that depends on a function $\phi(x)$, the condition that the value is stationary with respect to variations in ϕ is

$$\frac{dF}{d\phi} = 0. \quad (1.4)$$

This must be satisfied for all values of x . If there is a constraint that some other integral $\int G(\phi)dx$ has a fixed value, the stationary condition contains the constraint as a Lagrange multiplier,

$$\frac{dF}{d\phi} + \mu \frac{dG}{d\phi} = 0. \quad (1.5)$$

We now apply this to the Hartree-Fock energy, eq. (1.2), varying with respect to a wave function amplitude ϕ_a^* . Remembering that the wave functions were assumed to be normalized, we impose the constraint $\int \phi_a^* \phi_a d^3r = 1$ with a Lagrange multiplier. The multiplier will be denoted ϵ_a ; it looks exactly like the energy in the Schrödinger equation. The wave functions also have to be orthogonal as well, but it turns out

Table 1. Atomization energies of selected molecules

	Li ₂	C ₂ H ₂	20 simple molecules (mean absolute error)
Experimental	1.04 eV	17.6 eV	-
Theoretical errors:			
Hartree-Fock	-0.94	-4.9	3.1
LDA	-0.05	2.4	1.4
GGA	-0.2	0.4	0.35
τ	-0.05	-0.2	0.13

that it is not necessary to put in Lagrange multipliers to satisfy that condition. There is one more technical point in carrying out the variation. When the gradient of a function is varied, one first integrates by parts to move the gradient elsewhere in the expression. One must impose suitable boundary conditions on the function to carry out the integration by parts, and that must be remembered in solving the differential equations that result from the variation.

Without going through the steps I will just quote the result here. One obtains N equations for the amplitudes ϕ_a ,

$$-\frac{\hbar^2}{2m}\nabla^2\phi_a(\mathbf{r}) + \int \frac{e^2}{|\mathbf{r}-\mathbf{r}'|}n(\mathbf{r}')d^3r'\phi_a(\mathbf{r}) - \sum_b \int d^3r' \frac{e^2}{|\mathbf{r}-\mathbf{r}'|}\phi_a(\mathbf{r}')\phi_b^*(\mathbf{r}')\phi_b(\mathbf{r}) + V_{ext}(\mathbf{r})\phi_a(\mathbf{r}) = \epsilon_a\phi_a(\mathbf{r}). \quad (1.6)$$

These are the Hartree-Fock equations. It is interesting to see how well they do in making a theory of matter. In Table I is shown some energies calculated with eq. (1.6), taken from Refs. 1, 2. The entries in the table are atomization energies, which is the energy require to pull the cluster or molecule apart into individual atoms. Results are given for a simple atomic cluster, a simple molecule, and a set of molecules that are used as a testing ground for better theories. The mean absolute error in the atomization energies (energy difference between the molecule and the individual atoms in isolation) is 3 eV in the Hartree-Fock theory. The predicted binding of the Li₂ clusters is a factor ten too low, and another alkali metal cluster not in the table, Na₂, is incorrectly predicted to be unbound. We conclude that on a practical level Hartree-Fock is not accurate enough to be useful for chemistry or for computing cluster structures.

1.3. Homogeneous electron gas

We will see next time that the density functional theory makes use of the properties of the homogeneous interacting electron gas, and it will be useful to have on hand some analytic results. There is a systematic expansion of the energy of an electron gas accurate at high density. The first two terms are contained in the Hartree-Fock theory. They are the kinetic energy of a free Fermi gas, and its exchange energy. As part of the warmup, I will now derive them.

1.3.1. Free electrons

For the free electron gas eq.(1.6) is solved without the potential energy, and in a box (a cube of side L) with periodic boundary conditions. Since the Hamiltonian contains only the one-particle kinetic energy operator, the equation is separable into N one-particle problems. The solution are plane waves with discrete wave vectors \mathbf{k} chosen to fulfill the boundary conditions $\phi(x + L, y, z) = \phi(x, y, z)$, etc.,

$$\phi_{\mathbf{k}}(\mathbf{r}) = L^{-3/2} e^{i\mathbf{k}\mathbf{r}} \quad \text{where} \quad \mathbf{k} = \left(\frac{2\pi}{L} \right) \begin{pmatrix} n_x \\ n_y \\ n_z \end{pmatrix} \quad n_i = 0, \pm 1, \pm 2, \dots \quad (1.7)$$

According to the Pauli Principle each \mathbf{k} -vector can be occupied by two electrons. Thus the volume in k -space required for one electron is

$$V_k^0 = \frac{1}{2} \left(\frac{2\pi}{L} \right)^3 \quad (1.8)$$

and a sum over states can be replaced by an integral over \mathbf{k} according to

$$\sum_{\mathbf{k}} \rightarrow 2L^3 \int \frac{d^3k}{(2\pi)^3}.$$

The kinetic energy of a particle of wave vector \mathbf{k} is given by $\epsilon_{\mathbf{k}} = \hbar^2 k^2 / 2m$. Clearly the lowest energy state for a given number of electrons requires that the states are filled within a sphere in k -space, the Fermi sphere. Calling the radius of the sphere the Fermi wave number k_F , the number of particles can be expressed

$$N = 2L^3 \int_{k < k_F} \frac{d^3k}{(2\pi)^3} = L^3 \frac{k_F^3}{3\pi^2}$$

and the corresponding density n is given by

$$n = N/L^3 = k_F^3 / 3\pi^2.$$

The total kinetic energy of the electron gas is found by integrating the single-electron kinetic energy over the Fermi sphere,

$$T = 2L^3 \int_{k < k_F} \frac{(\hbar k)^2}{2m} \frac{d^3k}{(2\pi)^3} = \frac{L^3 \hbar^2 k_F^5}{10m\pi^2}$$

We shall later need the kinetic energy density as a function of particle density. Combining the last two equations one finds

$$t = \frac{T}{L^3} = \frac{3}{10} \frac{\hbar^2 (3\pi^2)^{2/3}}{m} n^{5/3} \quad (1.9)$$

1.3.2. Exchange energy

We evaluate the interaction in the Hartree-Fock approximation to find the next term in the energy of the electron gas. I will assume that the system remains uniform in the presence of the interaction. In general this should not be taken for granted; just because the Hamiltonian has some symmetry does not imply that the solutions do also. For the uniform solution, the wave functions remain plane waves. The next problem is that the Hartree term diverges because of the long range of the Coulomb interaction. The remedy is to include an external field to compensate, adding a positive background charge density equal in magnitude to the electron charge density. This is called the *jellium model*; in it the Hartree term is canceled exactly. That leaves the exchange energy given by

$$E_x = -\frac{1}{2}2L^6 \int_{k_F} \frac{d^3k}{(2\pi)^3} \frac{d^3k'}{(2\pi)^3} \int_L d^3r \int_L d^3r' \frac{e^2}{|\mathbf{r} - \mathbf{r}'|} \phi_{\mathbf{k}}^*(\mathbf{r}) \phi_{\mathbf{k}}(\mathbf{r}') \phi_{\mathbf{k}'}^*(\mathbf{r}') \phi_{\mathbf{k}'}(\mathbf{r}). \quad (1.10)$$

The factor of 1/2 comes from replacing the sum over orbital pairs by an unrestricted sum over orbitals. Next to it there is a single factor of 2 for spin because the two particles exchanged have to have the same spin wave function. It is easy to see how this integral will depend on the charge and on the density without going through the details of carrying it out. First, the factors of L will cancel out when the expressions for the plane wave states are inserted. The dimensionful quantities left are the electron charge squared, e^2 , and the Fermi wave number k_F . These have dimensions of energy-length and $(\text{length})^{-1}$, respectively. The only quantity that can be constructed from these with dimensions of energy density is $e^2 k_F^4$. The result of carrying out the integration must be that expression multiplied by a pure number. I won't carry out the integrals here but just give the result. The exchange energy density e_x as a function of number density is

$$e_x = \frac{E_x}{L^3} = -\frac{3}{4\pi} e^2 (3\pi^2)^{1/3} n^{4/3}. \quad (1.11)$$

Notice that the power of n is less than in the kinetic energy term. This suggests that the expansion one is making for the energy in terms of the density is a high-density expansion. Indeed, when one evaluates the third term in the systematic many-body theory, one finds it to be small compared to the previous terms in the high density limit. But there is a surprise at that order: the expansion is not a simple Taylor series in $1/n^{1/3}$, but is nonanalytic^a. For future reference, I will quote the full expansion up to that order:

$$e = 2.87 \frac{\hbar^2}{m} n^{5/3} - 0.74 e^2 n^{4/3} + \frac{e^4 m}{\hbar^2} (0.031 \ln(\hbar^2 n^{1/3}/m e^2) - 0.062) + \dots \quad (1.12)$$

^aThis was derived by Gell-Mann and Brueckner in 1957. ³

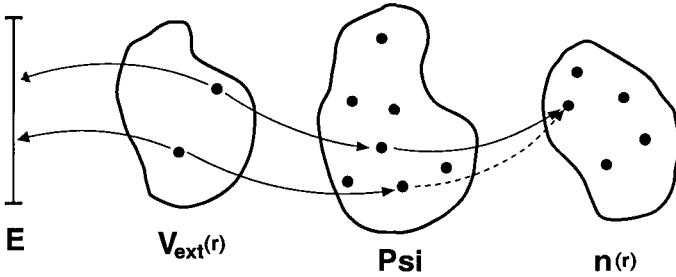


Fig. 1. Logic of the Hohenberg-Kohn theorem. The dashed mapping from a many-body wave function Ψ to a density $n(r)$ is not possible, given that another mapping exists.

2. What is density functional theory?

The Hohenberg-Kohn theorem states that a variational functional exists for the ground state energy of the many-electron problem in which the varied quantity is the electron density. In this section I will go through the proof and then give a simple example of a candidate density functional theory.

2.1. Hohenberg-Kohn theorem

We first separate the many-electron Hamiltonian into a part H_0 that depends only on the electron coordinates and a part V_{ext} that contains the electrons' interaction with external charges and fields. Referring back to eq. 1.1, H_0 contains the first two terms and V_{ext} is the last term. It should not cause any confusion to use the symbol V_{ext} both for the operator in the many-electron space and for the ordinary function of the coordinate. Let us call the ground-state wave function for this Hamiltonian Ψ . In principle we could then find the ground state energy $E = \langle \Psi | H_0 + V_{ext} | \Psi \rangle$ and the electron density in the ground state, $n(r) = \langle \Psi | \psi^\dagger(r) \psi(r) | \Psi \rangle$. These mappings are shown as the solid arrows in Fig. 1. We now ask the question of whether another Hamiltonian, differing only by the external field, could have the same ground state density. That situation would be represented by the dashed arrow in Fig. 1. This cannot happen if the ground state is nondegenerate. The proof is carried out by *reductio ad absurdum*. Suppose that a V'_{ext} and a Ψ' exist such that $n'(r) = n(r)$, with a ground state energy $E' = \langle \Psi' | H_0 + V'_{ext} | \Psi' \rangle$. If the ground state is nondegenerate, the other state must have a higher expectation value of the primed Hamiltonian,

$$\langle \Psi | H_0 + V'_{ext} | \Psi \rangle > E'$$

By adding and subtracting the expectation of V_{ext} on the left hand side, it can be rewritten to put the inequality in the form

$$E + \int n(r)(V'_{ext} - V_{ext})d^3r > E'$$

In deriving this, we also made use of the assumption that $n = n'$. The same reasoning can be carried out starting from the expectation values of the Hamiltonian $H_0 + V'_{ext}$

in both states. That gives the inequality

$$E' + \int n(r)(V_{ext} - V'_{ext})d^3r > E$$

Adding the two inequalities gives

$$E + E' < E + E'$$

which is a contradiction. Thus, either the states are degenerate or $n \neq n'$. Since the mapping of Ψ into n is one-to-one, its image in n is invertible. Let us call the functions of the image n_v (possible densities associated with Hamiltonians of the form $H_0 + V_{ext}$), and the mapping from densities back to wave functions $\Psi[n_v]$.

We are now ready for the main theorem. The Hohenberg-Kohn theorem states that the mapping of n_v to energies E defined by

$$E = \langle \Psi[n_v] | H_0 + V_{ext} | \Psi[n_v] \rangle$$

is a variational principle whose minimum is the ground state energy. Given the mappings, the proof is trivial. The energy is variational in the full space of wave functions, and thus must also be variational in a restricted space that includes the minimum. Note that the derivation gives no clue on how to construct the functional, nor does it guarantee that it is smooth enough to apply the variational equations 1.4 or 1.5.

2.2. A simple example: the Thomas-Fermi theory

The simplest example of a DFT, which I will now derive, is the Thomas-Fermi model electronic systems. Looking again at the Hartree-Fock energy function, eq. (3), we see that two of the four terms are already in the desired form, i.e. depending only on the density $n(\mathbf{r})$. These are the direct electron-electron interaction and the interaction with the external potential. That leaves the kinetic energy and the exchange energy to be approximated by a function or functional of density. The Thomas-Fermi theory emerges when we ignore the exchange energy and make the simplest possible approximation for the kinetic energy. For a slowly varying density function the kinetic energy density will only depend on the number density at the same position, Taking the specific function from the Fermi gas, eq.(1.9), we arrive at the kinetic energy functional

$$T[n(\mathbf{r})] = \int \epsilon(n(\mathbf{r}))n(\mathbf{r})d^3\mathbf{r} = \int \frac{3}{10} \frac{\hbar^2(3\pi^2)^{2/3}}{m} n^{5/3}(\mathbf{r})d^3\mathbf{r} \quad (2.1)$$

The sum of the kinetic and the potential energy terms will give us the total energy within the Thomas-Fermi approximation,

$$E[n(\mathbf{r})] = \int \left[\frac{3}{10} \frac{\hbar^2(3\pi^2)^{2/3}}{m} n^{5/3}(\mathbf{r}) + \frac{e^2}{2} \int \frac{n(\mathbf{r})n(\mathbf{r}')}{|\mathbf{r} - \mathbf{r}'|} d^3\mathbf{r}' + V_{ext}n(\mathbf{r}) \right] d^3\mathbf{r} \quad (2.2)$$

Note that the expression only depends on $n(r)$. In the next section we will apply the variational principle to find the Thomas-Fermi equation.

2.2.1. Variational equation of Thomas-Fermi theory

To find the ground state density function, one has to minimize the total energy functional for a fixed number of particles. This constraint is included by adding a term to the functional, $\mu \int n d^3r$, with μ the Lagrange multiplier. The variational problem is then expressed

$$0 = \delta E[n(\mathbf{r})] \quad (2.3)$$

$$= \delta \int \left[\frac{3}{10} \frac{\hbar^2 (3\pi^2)^{2/3}}{m} n^{5/3}(\mathbf{r}) + \frac{e^2}{2} \int \frac{n(\mathbf{r})n(\mathbf{r}')}{|\mathbf{r} - \mathbf{r}'|} d^3\mathbf{r}' + V_{ext}(\mathbf{r})n(\mathbf{r}) - \mu n(\mathbf{r}) \right] d^3\mathbf{r}$$

where the variation is to be taken with respect to $n(\mathbf{r})$. Eq. 1.5 then gives

$$\frac{\hbar^2}{2m} (3\pi^2)^{2/3} n^{2/3}(\mathbf{r}) + e^2 \int \frac{n(\mathbf{r}')}{|\mathbf{r} - \mathbf{r}'|} d^3\mathbf{r}' + V_{ext}(\mathbf{r}) - \mu = 0 \quad (2.4)$$

This is an integral equation for $n(\mathbf{r})$, but it can be converted into a differential equation which is easier to solve. This is done by defining a potential

$$V_e(\mathbf{r}) = +e^2 \int \frac{n(\mathbf{r}')}{|\mathbf{r} - \mathbf{r}'|} d^3\mathbf{r}'.$$

and seeing that the potential will be a solution of the Poisson equation^b,

$$\nabla^2 V_e(r) = -4\pi e^2 n(r). \quad (2.5)$$

We first use eq. (2.4) to express n as a function of V_e ,

$$n(\mathbf{r}) = \frac{1}{3\pi^2 \hbar^3} (2m(-V_{ext}(\mathbf{r}) - V_e(\mathbf{r}) + \mu))^{3/2} \quad (2.6)$$

Then substitute into the right hand side of eq. (2.5) to obtain

$$\nabla^2 V_e(\mathbf{r}) = -\frac{4e^2}{3\pi \hbar^3} (2m(-V_{ext}(\mathbf{r}) - V_e(\mathbf{r}) + \mu))^{3/2}. \quad (2.7)$$

2.2.2. Thomas-Fermi atom

Further simplification can be obtained if particular assumptions are made for the external potential V_{ext} . For a spherical external field such as that of an atom, the potential functions will only depend on the radius. The potential of the atomic nucleus, $V_{ext}(r) = -Ze^2/r$, can be included into eqns.(2.6,2.7) to yield a general formulation valid for arbitrary atomic Z . To analyze the atomic theory, it is convenient to define a dimensionless function $\phi(r)$ according to

$$\frac{Ze^2 \phi(r)}{r} = \frac{Ze^2}{r} - V_e(r) + \mu. \quad (2.8)$$

^bIn fact, the Poisson equation would be obtained immediately if one started from an energy function that has an explicit term for the electrostatic field energy.

Then the radial Laplacian operator reduces to a simple second derivative, and eq. (14) becomes

$$\phi''(r) = \frac{4e^3 Z^{1/2}}{3\pi\hbar^3} (2m\phi)^{3/2} r^{-1/2}. \quad (2.9)$$

The equation for the density is the same as before; in terms of the variable ϕ it is

$$n(r) = \frac{1}{3\pi^2\hbar^3} \left(\frac{2me^2 Z\phi}{r} \right)^{3/2}. \quad (2.10)$$

These equations can be found in textbooks as the general Thomas-Fermi equations for atoms. By taking into account that the electron potential must be finite at $r = 0$ one can fix one initial condition for ϕ , $\phi(0) = 1$. Since it is a second-order equation, another condition must be imposed. In practice one makes a guess at the initial slope $\phi'(0)$, integrates to large r , sees what the solution looks like. There are three cases to be considered. The first is that ϕ remains positive and finite over the whole range of r up to infinity. This is unphysical because eq. (2.10) would imply that the electron density was finite everywhere. The next possible is that ϕ goes through zero at some point r_0 , implying (eq. (2.10) again) that $n(r_0) = 0$. We can assume that the density remains zero for larger radii. Let us integrate the density to get the total number of electrons N ,

$$N = \int_{r_0}^{\infty} n(\mathbf{r}) d^3\mathbf{r}. \quad (2.11)$$

Then the potential outside of r_0 must be Coulombic and given by $-(Z - N)e^2/r$. Matching at r_0 gives the value of the chemical potential,

$$\mu = -\frac{(Z - N)e^2}{r_0}. \quad (2.12)$$

This defines the Thomas-Fermi model of an atom with N electrons and atomic number Z . The chemical potential is negative, implying that $N < Z$.

The last case in integrating the Thomas-Fermi equation is the boundary situation where the function ϕ only goes to zero asymptotically at large r . The chemical potential is zero in this case, and the integral of the electron density is equal to the nuclear charge. This defines the Thomas-Fermi theory of the neutral atom.

In all cases the Thomas-Fermi equations require a numerical solution. Not even in the neutral-atom case it can be calculated analytically. However, eq. (2.9) has one very nice feature for that case. Namely, there is no finite r_0 to fix the dimension of the atom, and all of the dimensional information is contained in the coefficient on the right hand side. The equation assumes the dimensionless form $\phi''(x) = \phi^{3/2}(x)/x^{1/2}$ if we make the change of variable to $r \rightarrow (3\pi/4)^{2/3}(\hbar^2/2me^2)x$ in eq.(2.9). Thus all neutral atoms are described by the same universal function $\phi(x)$.

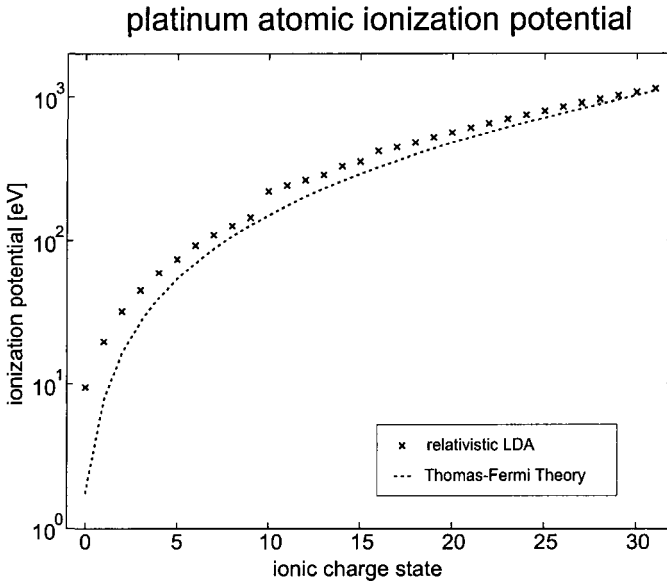


Fig. 2. Comparison of ionization potentials of platinum atoms. Dotted line is the Thomas-Fermi prediction; crosses mark the values from the Dirac-LDA theory.

2.2.3. An example

Let us see how well the Thomas-Fermi theory does for a heavy atom. I take as an example the Pt atom which has $Z = 78$. We will examine the ionization potentials starting from the neutral atom and going up to a charge $Q = Z - N = 30$. The Thomas-Fermi calculations are done in the way described in the previous section: one tries an initial condition, integrates, examines the charge, and from that refines the initial condition. For a given charge N the total Thomas-Fermi energy can be computed using the energy function eq. (2.2). The ionization potential of the ion is defined as a difference in the total energies; for charge Q $IP = E(N = Z - Q) - E(N = Z - Q - 1)$. Of course in the Thomas-Fermi theory N is a continuous parameter; we simply take the energy at the integer values. Experimentally, one only knows the ionization potentials for a few charge states. So for comparison purposes we also calculated the values using the more sophisticated Dirac-Hartree-LDA theory. The results are shown in Fig. (2). We see that the results come out quite well for high charge states, and the overall trend is reproduced. However the first ionization potential comes out poorly. Experimentally it is 9.0 eV and in the relativistic Hartree-LDA theory it is 9.5 eV, but in the Thomas-Fermi it is predicted to be only 1.8 eV.

Another failing of the Thomas-Fermi model is the complete absence of atomic shell effects. It may be seen in the Figure that there is a jump in ionization potentials between charges $Q = 9$ and $Q = 10$. This is due to the depletion of the $5d$ shell and the beginning ionization of the $5p$ shell. Shell effects such as this are

in fact beyond the scope of theories that ignore the wave character of quantum mechanics. Thomas-Fermi theory fails on another fundamental property of many-electron physics, namely the existence of molecules. It can be shown (Ref. 4) that all molecules would be unstable with respect to dissociation into isolated atoms, according to the energies calculated in the Thomas-Fermi theory. Again, this points to the need for explicit wave function mechanics. From the Figure one can also see that the Thomas-Fermi systematically underpredicts the ionization potentials. This is a deficiency that can in principle be remedied by the use of a more sophisticated energy function. We shall return to this point later.

3. Kohn-Sham theory

We saw in the previous section that explicit quantum mechanics is needed to make a theory that would reproduce the most elementary properties of matter. Kohn and Sham proposed, in essence, to put wave mechanics into the kinetic energy functional, but retain the density variable $n(\mathbf{r})$ elsewhere. Hartree-Fock theory gives us guidance on how to proceed. We take as the primary variational functions the orbitals of the Hartree or Hartree-Fock theory, and we calculate the kinetic energy accordingly. We also use these orbitals to determine the density. The interaction terms that can be expressed directly in terms of the density we keep, and we add another term, the exchange-correlation energy E_{xc} to take care of everything else. The resulting functional is

$$E_{KS}[\phi_1 \dots \phi_N] = \sum_a^N \frac{\hbar^2}{2m} \int d^3r \nabla \phi_a^* \cdot \nabla \phi_a + \frac{1}{2} \int d^3r \int d^3r' \frac{e^2}{|\mathbf{r} - \mathbf{r}'|} n(\mathbf{r}) n(\mathbf{r}') + E_{xc}[n] \\ + \sum_a \int d^3r V_{ext}(\mathbf{r}) |\phi_a|^2.$$

which is used together with the definition

$$n(\mathbf{r}) = \sum_a^N |\phi_a(\mathbf{r})|^2.$$

3.1. Local density approximation

Kohn and Sham proposed to treat the term E_{xc} as a simple integral over an energy density $e_{ex}(\mathbf{r})$, which in term is taken as an ordinary function of the local density, i.e. $e_{ex} = f(n(\mathbf{r}))$. This is called the local density approximation (LDA). The obvious choice for the function f is the corresponding energy density of the uniform electron gas. Since the kinetic energy is treated separately, the exchange-correlation energy is what is left over after taking away the first term in eq. (1.12). In fact, the idea to take the exchange energy from the electron gas was first attempted by Slater. Starting from the Fermi gas exchange energy density in eq. (1.11). Slater proposed to make a local density approximation by defining a two-body contact interaction

that would have the same energy density. Taking an interaction of the δ -function form $V(\mathbf{r}-\mathbf{r}') = v_0\delta(\mathbf{r}-\mathbf{r}')$, the many-body interaction energy density would be $v = 1/2v_0n^2$. Comparing with the required energy density associated with the exchange, Slater added to the Hartree Hamiltonian a two-particle contact interaction with a strength given by $v_0 = 3e^2(3/\pi)^{1/3}n^{-2/3}/2$. Then the Schrödinger equation would have an additional potential term given by

$$V_{Slater} = -\frac{3e^2}{2\pi}(3\pi^2n_e(r))^{1/3}.$$

THIS IS WRONG. Going back to the variational principle, one sees that the one-body potential should be defined by the variation of E_{xc} , i.e.

$$V_{xc}(r) = \frac{\delta e_{xc}}{\delta n} = -\frac{e^2}{\pi}(3\pi^2n_e(r))^{1/3}. \quad (3.1)$$

This is a factor 2/3 different from Slater's potential.

In practice, the LDA density functional theory takes the exchange-correlation energy from numerical calculations of the interacting electron gas. Many-body theory gives a few terms of the high-density expansion, but only numerical methods are reliable for the lower densities of interest. The classic reference is the Green's function Monte Carlo calculation of Ceperley and Alder, ⁵ who gave a table of energies of the homogeneous electron gas. After subtracting the kinetic energy of the free Fermi gas, the function is parameterized in a way suitable for taking the derivative needed in eq. 3.1. Such parameterizations give the "LDA" functional of density functional theory. It gives a considerable improvement over Hartree-Fock, as may be seen by the entries in Table 1. Alkali metal clusters have reasonable binding energies, and the errors in the atomization energies decrease by a factor of two. But this is still not accurate enough for chemical modeling.

3.2. Spin and the local spin density approximation

Up to now we have assumed that the electrons are all paired in the molecular orbitals: the electron density was calculated assuming two electrons occupy each spatial orbital, and the exchange-correlation energy was fit to the energy of an electron gas with equal number of up and down spin electrons. There is no reason why we can't treat up and down electrons separately, generalizing the theory to treat two (variationally) independent densities. Thus we define spin-up and spin-down densities n_\uparrow, n_\downarrow , and construct an exchange-correlation energy depending on both. The exchange part of the interaction is between electrons with the same spin projection, so the corresponding energy functional is a sum of two terms. Going through the same procedure we did to find the exchange interaction before, one finds the for the exchange energy density

$$e_x = -\frac{3}{4}\left(\frac{6}{\pi}\right)^{1/3}e^2(n_\uparrow^{4/3} + n_\downarrow^{4/3}) \quad (3.2)$$

The correlation energy of a spin-polarized electron gas has also been calculated and fit. The parameterization of Perdew and Zunger⁶ is often used; the spin-dependent correlation energy is about half the size of the spin-dependent exchange energy, for densities in the range of those occurring for conduction electrons in metals.

Eq. 3.2 has one feature that is obviously unphysical: it is not invariant under rotations. Suppose we have a system with the electrons polarized in the x -direction. The electron wave function then has equal amplitudes of up and down spin, and the spin-up and spin-down densities are equal. Thus the formula would treat this incorrectly as an unpolarized system. This can be easily fixed by taking as density variables the entire spin density matrix.⁷ The eigenvalues of the matrix are invariant under rotations, and the energy functional depends only on the eigenvalues. I will show an application later on.

3.3. The generalized gradient approximation

An obvious problem of the LDA is that the single-particle potential does not have the correct asymptotic behavior. The electron potential in a neutral cluster should behave as $-e^2/r$ for large separation of the electron from the cluster. But in the LDA the Coulomb potential is calculated with all the electrons and thus vanishes outside the cluster. This makes the LDA unreliable for calculating ionization potentials from the Kohn-Sham eigenvalues.

There is another argument why one should not trust the absolute numbers of the Kohn-Sham eigenvalues. Let us imagine starting with the full normalized wave function of a particle in its orbital, and take away probability a little bit at a time. Since quantum mechanics is a linear wave theory, the energy cost is the same to take away a bit of the probability, independent of how much has been taken away already. But the self-interaction and exchange terms are nonlinear functions, and the energy in the Kohn-Sham theory does depend on how much probability is left^c. This function behaves as $-aP^{4/3} + bP^2$. The cancellation of the self-energies comes about by having $a \approx b$. But Kohn-Sham potential comes from the derivative which is positive near $P = 1$.

As an example of how this works out in a physical example, we calculated the ionization potential (IP) of the silver atom both ways. According to Hartree-Fock theory, the Ag atom has a single electron in an s orbital, with an unoccupied p orbital just above and a fully occupied d orbital just below. Thus the IP should correspond to the energy of the s -orbital. Table 2 shows the experimental ionization potential (IP) compared to the Kohn-Sham eigenvalue. You see that it is predicted to be more weakly bound than is the actual IP, and the error is quite large (40%).

^cThis gives rise to a real pathology of the LDA functional, that a free electron comes out to be self-bound in its exchange potential

Table 2. Atomic properties of the Ag atom in LDA.

	IP	First excited state
Experimental	7.75	3.74
Kohn-Sham: eigenvalues	$\epsilon_s = 4.6$	$\Delta\epsilon = 3.9$
total energies	8.0	4.1

What about the other method? The line labeled “total energies” was calculated as a difference between energies of the neutral atom and the singly-charged ion, i.e.

$$IP = E(\text{Ag}) - E(\text{Ag}^+). \quad (3.3)$$

The table shows that the error is only 3% when the IP is calculated this way.

Becke⁸ proposed a fix to get the $-e^2/r$ asymptotic potential by adding a term to the energy functional that depends on the gradient of the density, $\nabla n_e(r)$. His proposed form works amazingly well. This is the “generalized gradient approximation”, GGA. From Table 1, we see that energies can be calculated to an accuracy of tenths of an eV. Further improvements may be possible. The Kohn-Sham energy functional depends on the nonlocal quantity

$$\tau = \sum_i |\nabla\phi_i|^2$$

in the kinetic energy term. One could think of using other functional dependencies on τ ; an example is given in the last line of Table 1.

The functional that is most popular in quantum chemistry is called the “B3LYP”. Its popularity derives in part from the fact that it is a option in a widely distributed computer program for quantum chemistry calculations. Unfortunately, the prescription is quite *ad hoc*, taking pieces from many sources include Hartree-Fock, the local spin density approximation, and the GGA. It is not even easy to find its definition without going to the original literature for the individual terms (e.g. Ref. 9).

Later on, I will show some calculations that use the GGA prescription of van Leeuwen and Baerends.¹⁰ They write the exchange-correlation potential as

$$v_{xc}(\mathbf{r}) = -\beta n^{1/3}(\mathbf{r}) \frac{x^2(\mathbf{r})}{1 + 3\beta x(\mathbf{r}) \sinh^{-1}(x(\mathbf{r}))}$$

where $x = |\nabla n|/n^{4/3}$.

4. Numerical methods for the Kohn-Sham equation

The DFT is conceptually quite simple, but its success is in part due to the development of efficient methods to solve the Kohn-Sham equations. The algorithms may be classified by how the orbital wave function is represented. The traditional approach in quantum chemistry is to use a basis set of analytic functions centered on each atom. Gaussian basis sets are very popular because the Coulomb integrals

Table 3. Symbol definitions for quantities pertaining to the computational effort required to solve the Kohn-Sham equations of DFT.

	Symbol	Meaning
N	N_ϕ	dimension of vector representation ϕ
	N_r	real-space points
	N_k	reciprocal-space points
	N_e	number of electron orbitals
	N_c	unoccupied orbitals
M	M_H	nonzero elements in H matrix row
	M_{it}	iterations in conjugate gradient method
	M_T	time steps
	M_ω	number of frequencies

can be evaluated exactly. Such representations have several disadvantages, however. The basis is not orthogonal, which makes it somewhat inconvenient to use. To establish convergence one has to have the flexibility to add additional functions, and this may not be easy to do, for example when one is describing weakly bound electrons. The other kind of representation is to use plane waves, i.e. a mesh in momentum space, or a mesh in coordinate space. These representations suffer from the disadvantage that the required mesh has a much finer granularity close to the nuclei than far away. It is not yet practical to deal with the full range of energy scales in the atomic problem with a uniform mesh. The way out for condensed matter theorists is to replace the nuclear potential by a much smoother pseudopotential, so that a relatively coarse grid can be used everywhere. There is much art to the construction of pseudopotentials, and I will not discuss them in detail. A popular prescription for constructing pseudopotentials was formulated in Ref. 11; a program to generate pseudopotentials this way can be download from the web site <http://bohr.inesc.pt/~jlm/pseudo.html>. Another more recent prescription together with tables of the pseudopotential parameters can be found in Ref. 12.

It is very useful to understand the computation cost of the various algorithms for solving the equations. To quantify that as much as possible, I have defined some numerical quantities in Table 3. Quantities which increase with the size of the system are denoted by the symbol N with some subscript. Other quantities which may be large but are independent of the system size are denoted by the symbol M .

Part of solving the Kohn-Sham equations is to construct a potential V_e for the electron-electron interaction, given the density $n(\mathbf{r})$. This requires solving the Poisson equation, which can be done efficiently in several ways. Very straightforward is to use the Fast Fourier Transform. This converts a function represented on a real space grid to the Fourier space, and it requires about

$$5N \log_e N$$

floating point operations to make the three-dimensional transform, with $N = N_r$ or N_k . Let us call the transform $\tilde{\phi}(k) = F\phi(r)$. The method achieves its efficient

by representing the matrix F as a product of sparse matrices F_i , $F = \prod_i F_i$. To solve the Poisson equation $\nabla^2 \phi = -4\pi n$, one simply performs the operations in the formula

$$\phi(r) = F^{-1} \frac{4\pi}{k^2} F n(r),$$

requiring 2 FFT's per cycle. As its name implies, the FFT is fast. But it also has some disadvantages. The full efficiency is available only for particular meshes; the largest routinely in use is $(128)^3 \approx 2 \times 10^6$ points. Also, as a finite Fourier transform, it imposes a periodicity on the system. This is no problem for the condensed matter theorists calculating properties of crystals, but for finite systems the spurious "superlattice" sometimes requires one to use large boxes that would be the case for a finite system. For ways to cope with this problem, see Ref. 13.

There is another method that is well suited to finite systems, and is also very efficient. That is the *multigrid method*, which you can find described in textbooks¹⁴ or in a review article on numerical methods for density functional theory.¹⁵ The method uses a finite difference formula in coordinate space to represent the Laplacian operator. You all are familiar with the three-point difference formula, $\nabla_x^2 \phi \Big|_{x_0} \approx (\phi(x_0 + \Delta x) + \phi(x_0 - \Delta x) - 2\phi(x_0))/\Delta x^2$. Higher order approximations are more efficient in that they allow one to use a coarser mesh for a given level of accuracy. Also important to the multigrid methods the use of a sequence of coarser meshes to deal with the long-wavelength part of ϕ . Without multigridding, the standard equation-solving techniques converge very slowly, requiring a large number of iterations. In practice, the multigrid method reduces the error in an approximate solution by a factor of two or so with each cycle of multigridding. Its speed is comparable to the FFT.¹⁵ Given the Hartree potential, the next task is to solve the three-dimensional Schrödinger equation. With the large dimensions of the spaces required to represent the wave functions, only iterative methods are practical. These operate by refining the wave function. At the heart of any method is the operation of applying the Kohn-Sham operator H_{KS} to a wave function. As a matrix multiplication, the operation requires of order N_ϕ^2 floating point operations per wave function. Taking into account that the number of electrons grows with the size of the system, the operation scales with system size as $N_e N_\phi^3$. This would be very slow in practice. There are several algorithms that only require of the order of N operations per electron.

The one used by Chelikowsky *et al.*¹⁶ and by Yabana and Bertsch¹⁷ takes advantage of the coordinate space representation. The potential is local or nearly local, so it only takes N_r operations to construct the vector $V\phi$ starting from V and ϕ as separate N_r -dimensional arrays. The kinetic energy is represented as a difference operator as in the multigrid method, giving a sparse matrix in the \mathbf{r} -representation. The operational count is thus $N_r M_H$ where M_H is the number of nonzero rows in the Hamiltonian. The FFT is also often used to perform the operation $H_{KS}\phi$. In what is called the split operator technique, the potential energy is evaluated in

coordinate space and the kinetic energy in reciprocal space, e.g.

$$H_{KS}\phi\Big|_r = -F^{-1}\frac{k^2}{2m}F\phi(r) + V_{KS}(r)\phi(r).$$

One also has a choice of methods for the iterative refinement of the wave function. The two main methods are the imaginary time propagation and the conjugate gradient method. The imaginary time propagation simulates the operator $\exp(-\tau H)$, which when applied to a wave function, will damp the higher energy components and enhance the lower energy components. The conjugate gradient method is a workhorse for any kind of problem with many variables and equations to be satisfied simultaneously. Besides the iteration to get the wave function, there is an iteration on the potential. Unfortunately, the kinetic energy operator has too large a range of eigenvalues to make either method rapidly convergent. There is a technique to improve the convergence, called preconditioning. Here one modifies the operator to reduce the amplitude of high momentum components in determining the correction to be applied in an iteration cycle. This is most easily done in wave vector space, but it has been applied also in real space using multigrid method (see Ref. 18).

I give as an example the calculation of the ground state of a ring of 20 carbon atoms using the Yabana-Bertsch code (available at <http://www.phys.washington.edu/bertsch>). The code uses the coordinate space representation and the 9-point difference formula for the kinetic energy operator. The other numerical parameters for the calculation are very simple to report. The wave functions were calculated in a cylindrical volume of $1,500 \text{ \AA}^3$. The mesh spacing was 0.3 \AA , giving $N_r \approx 56,000$ mesh points. The number of occupied electron orbitals is $N_e = 40$ for the C_{20} cluster. Namely, there are 4 valence electrons per carbon atom, and the orbitals are doubly occupied, giving $20 \times 4/2 = 40$ altogether. The core electrons of the carbons are only included implicitly in constructing the pseudopotential.

With a 9-point difference formula, the number of nonzero elements in the operator matrix is $M_H = 25$. This does not include the computation of the nonlocal parts of the pseudopotential, but that does add significantly to the total number of operations. In the code, the conjugate gradient method is used to extract the orbital wave functions, using five calls to the $H_{KS}\phi$ operation per orbital iteration. There does not seem to be an easy way to estimate the number of iterations required. For the case here, $M_{it} = 100$ gave convergence to a meV on the occupied orbital energies. Combining these numbers, one finds of the order of $5M_{it}M_HN_rN_e \approx 30 \times 10^9$ arithmetic operations. Our computer can do arithmetic operations at a pipelined speed of $0.2 \times 10^9 \text{ s}^{-1}$, giving a time of 150 seconds. In fact about twice as much time is spent in the subroutine. This shows that memory transfer also has a significant impact on the running speed.

4.0.1. Exact exchange

It is now easy to see why one avoids making an explicit calculation of the exchange interaction. The exchange term in the Hartree-Fock equation has the following form

$$H_{ex}\phi)_{a,r} = - \sum_b \int d^3r' \frac{e^2}{|\mathbf{r} - \mathbf{r}'|} \phi_a(\mathbf{r}') \phi_b^*(\mathbf{r}') \phi_b(\mathbf{r}).$$

Since there are two indices of orbitals and two position variables, the naive computational cost is proportional to $N_e^2 N_r^2$. This would be very time-consuming to compute, but it can somewhat ameliorated. One can use a Poisson solver to find the potential field

$$V_{ab}(r) = \int d^3r' \frac{e^2}{|\mathbf{r} - \mathbf{r}'|} \phi_a(\mathbf{r}') \phi_b^*(\mathbf{r}').$$

The computational cost here is $N_e^2 N_r M_{it}$. The second multiplication to get the exchange term is insignificant, giving an overall scaling as N^3 . In contrast, with the LDA or GGA, the exchange potential is just a local function of position with computational cost scaling as $N_e N_\phi$. In fact, the computer speed here is actually limited by memory access rather than arithmetic.

4.0.2. $\mathcal{O}(N)$ methods

There is much discussion now about methods to solve the Kohn-Sham equation that have a computational cost that increases only linearly with the size of the system. Various approaches are discussed by Goedecker in his review article.¹⁹ The basic issue is how to avoid the N^2 cost of computing N_e wave functions on a basis of size N_ϕ . There is a way around when one recognizes that the orbitals are not really the physical objects of the theory. Rather the physical quantity is the single-electron density matrix, $n(r, r')$, constructed from the orbitals. At least in insulators, this function goes to zero quickly as $|r - r'|$ becomes large. Thus, representing the density matrix requires one index r to have N_r values but the other index can be restricted in a way that is independent of N . I will just briefly mention two of the approaches that follow this line. The first is to use $n(r, r')$, suitably restricted, as the variational function. One can't just take the Kohn-Sham energy $E_{KS}[n(r, r')]$ by itself as the functional to be varied, because $n(r, r')$ must also respect the Pauli principle: not all $n(r, r')$ are compatible with an antisymmetrized many-electron wave function. This is taken care of in the orbital approach by constructing n from N_e orthogonal orbitals. Considering the density matrix as an operator, $\langle r | \hat{n} | r' \rangle = n(r, r')$, its characteristic properties is that it is a projection operator, with N_e eigenvalues equal to one and the rest equal to zero. Now suppose we have a trial density matrix that doesn't satisfy this projector property. We can drive its eigenvalues to one or zero by using the minimization principle $\pm \text{Tr} (3\hat{n}^2 - 2\hat{n}^3)$. We want to drive the orbitals below the Fermi energy to eigenvalue $n_i = 1$, and the orbitals above to $n_i = 0$.

This is accomplished by the variational principle

$$\text{Tr} \left((H_{KS} - \mu I)(3\hat{n}^2 - 2\hat{n}^3) \right).$$

where μ is the Fermi energy.

A related $\mathcal{O}(N)$ approach is to keep an orbital representation, but restrict the domain of each orbital to some neighborhood. Again, satisfying the Pauli principle is nontrivial. Since the orthogonality must be retained at least as an approximation, constraints must be introduced into the calculational method. A method that seems to be successful²⁰ is as follows. First, one puts the Fermi energy into the Hamiltonian as above, $H'_{KS} = H_{KS} - \mu I$. Second, one adds a term to drive the orbitals to orthonormality. A variational principle that can do this is

$$2 \sum_i \langle i | H'_{KS} | i \rangle - \sum_{i,j} \langle i | H'_{KS} | j \rangle \langle i | j \rangle.$$

The number of orbitals in the sums over i, j must be larger than N_e . The second term obviously doesn't have any effect if the orbitals space is complete, since then the Kohn-Sham orbitals are orthogonal and the variation of that term gives zero contribution to the Kohn-Sham operator. When the orbitals have appropriately restricted domains, the overlaps with a given orbital i will be zero except for a limited number of other orbitals j , and the number of basis amplitudes will be also be limited in the integrations. This make the method $\mathcal{O}(N)$, but does not guarantee that it convergences in a controlled way to the exact solution, or indeed that it convergences at all to the sought solution. The second method is farther along computationally,²¹ but more experience is needed to assess the reliability of these approximations.

5. Some applications and limitations of DFT

Since I have already discussed the predictive power of the DFT for molecules and clusters, this section only mentions other applications. At the end I mention some limitations arising from the implicit treatment of correlation effects.

5.1. Two examples of condensed matter

Here I will show you the results for crystalline silicon and iron, two materials of great importance in technology. The first properties a theory should be able to reproduce the structure of the element, namely its crystallographic form and the lattice size, and its binding energy. Iron has an additional complication that it is ferromagnetic, and the theory should reproduce the magnetic moment as well.

The properties of bulk silicon are shown in Table 4, according to the LDA calculations of Ref. 22 and 23. The LDA gives the correct crystal symmetry, and one can see from the table that the lattice constant is well reproduced. The bulk modulus can be calculated by find the energy of the material as a function of assumed lattice spacing. This also comes out very well. A property that comes out

much poorer is the electronic band gap. This may be defined either as the difference between electron removal and electron addition energy, or as the difference between Kohn-Sham eigenvalues for the highest occupied and the lowest unoccupied orbitals. In an infinite system these quantities are the same.

Table 4. Ground state properties of Si in the LDA, ^{22,23} compared to experiment.

Property	LDA	Experimental
lattice constant	5.42	5.42 Å
bulk modulus	0.96	0.99 MBar
band gap	0.52	1.17 eV

In the case of iron, there are important differences in the predicted structures between the LDA and the GGA theories. ²⁴ Table 5 shows these quantities for iron, both theoretically and calculated with the DFT. We see that the LDA fails the first test of the theory. Iron has a body-centered cubic structure, but the LDA has a lower energy for the hexagonal closed packed structure. On the other hand, the GGA gives the right structure and even comes very close on the lattice constant.

Table 5. Metallic Iron: an example of DFT. Theory is from Refs. 25, 26.

Property	Exp.	LDA	GGA
Crystal symmetry	bcc	hcp	bcc
Lattice constant a_0	2.87 Å	-4%	-0.5%
Cohesive energy	4.28 eV	+50%	+20%
Bulk modulus	1.68 Mbar	+40%	-8%
Magnetization	2.22 μ_B	-8%	+5%

The DFT correctly predicts the ferromagnetism of iron if the functional includes the spin-dependence interaction of the LSDA. As one can see from the table, the net spin per atom comes out rather well for both versions of the functional. The ferromagnetism of iron is rather simple in that the spin alignment is the same on each atom and one only needs to consider densities of spin up and spin down electrons. Other ferromagnetic materials have a more complicated spin structure, with the orientation of the spin depending on position. For these systems one would need to use the generalized spin functional to have the possibility of noncollinear spin alignment. In our group in Seattle we calculated the spin alignment in small cobalt clusters and found generalized spin functional gave a predicted noncollinear alignment. ²⁷

5.2. Vibrations

The DFT should also be applicable to vibrational properties. Recall that the DFT is a theory of the electronic ground state for an arbitrary external potential. Thus

we can displace the nuclei from the equilibrium positions and find the energy of the distorted structure. Table 5 shows the bulk modulus of iron calculated this way and compared to experiment. The error is large with the LDA but is only 8% with the GGA functional. Taking the DFT energy as a potential energy in the equations for vibrational motion, one can easily calculate the phonon dispersion relation for bulk systems. An 8% error in the force constant becomes a 4% error in the sound velocity, because of its quadratic relationship to the force constants.

In general, the DFT also works quite well for molecular vibrations. As an example I show some calculations of the infrared-active vibrations in the fullerene C_{60} . This is an example of historical interest, because the vibrational spectrum was one of the convincing early pieces of evidence that C_{60} had icosahedral symmetry. There are $60 \cdot 3 - 6 = 174$ vibrational modes in a molecule with 60 atoms, and if there were no symmetries they could all be excited by photon absorption. However, with icosahedral symmetry, only four of the modes have nonzero dipole matrix elements. Observation of exactly four modes in the infrared absorption spectrum was one of the convincing evidences of that structure when Krätschmer and Huffman first synthesized it in bulk.²⁸

Table 6. Excitation energies of C_{60} infrared-active vibrations (T_{1u}).

Mode	1	2	3	4
Experimental	0.065 eV	0.071	0.147	0.177
LDA error				
Ref. 29	-2%	-2%	+2%	+10%
Ref. 30	-3%	-7%	-8%	-7%

To calculate the modes, one first computes the potential energy surface as a function of displacement of the atoms from their ground state positions. Diagonalizing the Hessian matrix (the quadratic expansion of the potential energy surface) gives the normal modes and their frequencies. The results of three different LDA calculations are shown in Table 6. The agreement with experiment is impressive, with mean absolute relative error on frequency only 4%. A more demanding test of the theory is the transition strength associated with the vibrations. The accuracy here is perhaps only a factor of two.²⁹ But that is a great improvement over previous theories that were completely unreliable.

5.3. NMR chemical shifts

All the applications so far only requires energies or electron densities. There are other properties, more closely related to the electron wave function, that are better described by DFT than by Hartree-Fock theory. One of these is the current induced by an external magnetic field. We add a magnetic field to the energy functional by

including the gauge field \vec{A} in the kinetic energy operator,

$$\int d^3r \frac{\hbar^2}{2m} \left(-\frac{\nabla}{i} \psi^\dagger - e\vec{A}\psi^\dagger \right) \cdot \left(\frac{\nabla}{i} \psi - e\vec{A}\psi \right)$$

and adding a term representing the field energy associated with \vec{A} ,

$$\frac{1}{8\pi} \int d^3r |\nabla \times \vec{A}|^2.$$

The variation $\delta E_{KS}/\delta\phi_i^*$ then gives Kohn-Sham equations with the additional terms

$$\frac{e^2}{mc^2} |A|^2 \phi_i + \frac{e}{mc} \vec{A} \cdot \nabla \phi_i.$$

The variation with respect to \vec{A} gives the Maxwell equation relating the magnetic field $\vec{B} = \nabla \times \vec{A}$ to the current, where the current is defined by

$$\frac{\delta T}{\delta \vec{A}} = \frac{e}{mc^2} \vec{A} n + \frac{e}{m} \sum_i (\phi_i^* \nabla \phi_i - (\nabla \phi_i^*) \phi_i).$$

The current generates an additional magnetic field that weakly screens the external field. The fields at the nuclei are observable in nuclear magnetic resonance, and this screening gives rise to so-called chemical shifts of the NMR frequencies. Typically these are small, only hundredths of a percent, but they are easily measured and are characteristic of the chemical environment of the nucleus.

The DFT was compared with Hartree-Fock in Ref. 31. The calculations were done in an atomic orbital basis, which is far from trivial to use when dealing with gauge fields. I will just mention the results here, for the proton NMR shift in three molecules (HF, H₂O, CH₄). The proton chemical shift is of the order of 30×10^{-6} , and all the methods came within a few percent in the three cases. However, what is more interesting is the relative shift from one environment to another. These numbers are of the order 1×10^{-6} . The Hartree-Fock is found to be only accurate to a factor of two on the relative shifts, while the DFT is considerably better with only 20% errors. Interestingly, the ordinary LDA is as good or better than the GGA here.

6. Limitations of DFT

In some ways, the Kohn-Sham theory tries to capture the effects of correlations without building them explicitly into the wave function. There are certain systems and properties where explicit treatment of the correlations is needed, and we mention these before going on to discuss dynamics. Two well-known phenomena rely on correlations for their existence, namely superconductivity in bulk matter and the Van der Waals interaction between molecules. The van der Waals interaction is an attraction between particles that falls off as $1/r^6$ at moderately large distances. It is due to fluctuations in dipole fields associated with electronic transitions. Thus it is completely absent from a theory that represents the electron wave function

by a single Slater determinant. I want to show here how one could view density functional theory in a way that would make it natural to encompass the van der Waals interaction. Let us go back to eq. (1.12), the many-body theory expansion of the energy of the electron gas. The third term gives the contribution of correlations; in perturbation theory it has the second-order expression

$$\sum_{ii'} \sum_{cc'} \langle ij | \frac{e^2}{|\mathbf{r} - \mathbf{r}'|} | cc' \rangle^2 \frac{1}{\epsilon_i + \epsilon_{i'} - \epsilon_c - \epsilon_{c'}}.$$

The van der Waals interaction is obtained if one replaces the full Coulomb interaction in this expression by a dipole-dipole approximation

$$\frac{e^2}{|\mathbf{r} - \mathbf{r}'|} \approx \frac{e^2}{|\mathbf{R} - \mathbf{R}'|} + \frac{e^2(\mathbf{r} - \mathbf{R}) \cdot (\mathbf{r}' - \mathbf{R}')}{|\mathbf{R} - \mathbf{R}'|^3},$$

where \mathbf{R}, \mathbf{R}' are the centers of the two atoms and the integrations are restricted appropriately. One way to incorporate the van der Waals in the DFT would be as follows. Separate the Coulomb interaction into two parts, one containing the long wavelength components and the other the short wavelength components. In the DFT, incorporate the short-range Coulomb interaction into a local density approximation. For the long range part, calculate the second order perturbation explicitly. In this way the full interaction would be accounted for, but the van der Waals term would arise naturally.

Correlation effects are also hard to ignore in systems with a high density of states near the Fermi level. Then there is much configuration mixing, and the basic DFT approximation taking a single configuration to generate the density is not reliable. This suggests that one use the density functional theory to find the optimal orbitals in a set of configurations, and use other methods to improve the many-particle wave function by taking the configuration mixing into account. As with the van der Waals interaction, there is a conceptual difficulty in separating the part of the interaction that is treated by the LDA functional and the part that is treated by configuration mixing. A pragmatic approach is to ignore the overcounting and take $\frac{\delta H_{KS}}{\delta n}$ as a two-particle operator that can mix configurations. One such hybrid theory is called "LDA+U".³² The LDA is used to construct orbitals, but allows the wave to mix orbitals by an simplified interaction term on each site. That is called the "U". One finds that such an extension is essential for describing the phase diagram of metallic plutonium.³³ Another theory of this kind is called "dynamic mean field theory". It has also been applied to the metallic plutonium problem.³⁴

7. Time-dependent density functional theory: the equations

Schrödinger proposed two equations in his original paper, the eigenvalue equation for static properties and the time-dependent equation for the dynamics. But the left-hand side of both equations was the same. The situation is the same for dynamic theories based on Hartree-Fock or DFT. The theories may be derived from the

time-dependent variational principle,

$$\delta \int dt \langle \Psi | H - i \frac{\partial}{\partial t} | \Psi \rangle = 0. \quad (7.1)$$

Taking Ψ to be a Slater determinant and varying with respect to $\phi_i^*(r, t)$, one obtains the time-dependent Hartree-Fock equations, first proposed by Dirac.³⁵ The corresponding equations for DFT are the time-dependent Kohn-Sham equations,

$$H_{KS} \phi_i = i \frac{\partial}{\partial t} \phi_i. \quad (7.2)$$

There are several properties of the TDDFT that make it very attractive as a theory of electron dynamics. The theory automatically satisfies two important conservation laws, conservation of energy and the equation of continuity. To prove energy conservation in the TDDFT, take the derivative of the energy and expand using Eq. (7.2):

$$\begin{aligned} \frac{dE_{KS}}{dt} &= \sum_j \int d^3r \left(\frac{\delta E_{KS}}{\delta \phi_j^*} \frac{\partial \phi_j^*}{\partial t} + \frac{\delta E_{KS}}{\delta \phi_j} \frac{\partial \phi_j}{\partial t} \right) \\ &= \sum_j \int d^3r \left((H_{KS} \phi_j)(i H_{KS} \phi_j^*) + (H_{KS} \phi_j^*)(-i H_{KS} \phi_j) \right) = 0. \end{aligned}$$

To derive the equation of continuity, we start from the expression for the density, $n(r) = \langle \Psi | \psi^\dagger(r) \psi(r) | \Psi \rangle$, taking its time derivative. If Ψ were the exact wave function, the time derivative may be evaluated using the solution of the many-particle Schrödinger equation,

$$\begin{aligned} \frac{dn(r)}{dt} &= \langle \partial_t \Psi | \psi^\dagger(r) \psi(r) | \Psi \rangle \langle \Psi | \psi^\dagger(r) \psi(r) | \partial_t \Psi \rangle \\ &= i \langle (H \Psi) | \psi^\dagger(r) \psi(r) | \Psi \rangle - i \langle \Psi | \psi^\dagger(r) \psi(r) | H \Psi \rangle = i \langle \Psi | [H, \psi^\dagger(r) \psi(r)] | \Psi \rangle. \end{aligned}$$

We now assume that the Hamiltonian is local except for the kinetic energy operator T . Then the potential terms in the Hamiltonian commute with the density, and we only need to evaluate the kinetic energy commutator, $[T, \psi^\dagger(r) \psi(r)]$. It may be simplified using the fermionic anticommutator relations and the definition of derivatives as limits of differences. The result can be expressed in terms of the momentum density operator $\vec{p}(r)$, defined as

$$\vec{p}(r) = \frac{1}{i} (\psi^\dagger(r) (\nabla \psi)_r - (\nabla \psi^\dagger)_r \psi(r)).$$

It is also convenient to define the particle current, $\vec{j}_p = \vec{p}(r)/m$. The commutator of the density operator and the kinetic energy operator is then given by

$$[T, \psi^\dagger(r) \psi(r)] = \frac{i}{m} \nabla \cdot \vec{p}(r) = i \nabla \cdot \vec{j}_p.$$

Combining the above results and taking the operator expectation value in the wave function Ψ , we obtain the equation of continuity,

$$\frac{dn(\mathbf{r})}{dt} = -\nabla \cdot \langle \vec{j}_p(\mathbf{r}) \rangle.$$

This derivation assumed that Ψ was the exact wave function. In TDDFT, the wave function is given by Eq. (7.2), but the proof can still be carried out in the same way. The particle current will then have the expectation value

$$\langle \vec{j}_p \rangle = \frac{1}{im} \sum_j (\phi_j^* (\nabla \phi_j(\mathbf{r}))_r - ((\nabla \phi_j)_r)^* \phi_j(\mathbf{r})).$$

The fact the TDDFT satisfies the equation of continuity means that it will have the correct short-time behavior for the response of the system to external perturbations. This will be discussed in more detail below.

7.1. Optical properties

The most important application of the TDDFT is to the optical properties of molecules, atomic clusters, and condensed matter. In this section I will summarize for future reference a number of useful formulas for dealing with small systems. Here by small, I mean the dimension of the particle is much less than the wavelength of the photon. Then the electric dipole field dominates the interaction, and the optical response can be described with the dynamic polarizability $\alpha(\omega)$. Physically, we may come to the definition of alpha by asking the question, what is the form of an energy functional for a small finite system coupled to an external electric field? Expanding in powers of the field, we have the leading electric field-dependent terms,

$$\vec{d} \cdot \mathcal{E} + \frac{1}{2} \sum_{ij} \alpha_{ij} \mathcal{E}_i \cdot \mathcal{E}_j + \dots$$

The first term vanishes if the system does not have a dipole moment \vec{d} . The coefficients α_{ij} define the polarizability tensor. If the system has a high symmetry or if one is content with the average over angles, the second term can be written $\frac{1}{2} \alpha \mathcal{E} \cdot \mathcal{E}$ with $\alpha = \sum_i \alpha_{ii}$. The polarizability has a dimension of volume, which can be easily seen by comparing the energy expression with that for the electric field energy, $(1/8\pi) \int d^3r |\mathcal{E}|^2$.

Applying time-dependent perturbation theory for the field $x\mathcal{E}_0 \exp(-i\omega t)$, the polarizability in the x direction may be calculated as

$$\alpha_{xx}(\omega) = \frac{e^2}{\hbar} \sum_a \left| \langle 0|x|a \rangle \right|^2 \left(\frac{1}{-\omega - i\eta + \omega_a} + \frac{1}{\omega + i\eta + \omega_a} \right), \quad (7.3)$$

with a labeling excited states. The polarizability also has an equivalent definition as the linear coefficient of the field in the dipole moment of the system in an external

electric field,

$$e(x) = - \sum_i \alpha_{xi} \mathcal{E}_i + \dots \quad (7.4)$$

The imaginary part of the dynamic polarizability is directly related to the photon absorption cross section σ_{ab} . The relation is

$$\sigma_{ab} = \frac{4\pi\omega}{c} \text{Im} \alpha(\omega).$$

Under certain conditions the dielectric function of an extended medium is related to the polarizability of its constituents. This is the Clausius-Mossotti relation:

$$\epsilon(\omega) = \frac{1 + 8\pi\alpha n_0/3}{1 - 4\pi\alpha n_0/3}.$$

Here n_0 is the density of the polarizable particles. The conditions for validity of the formula are: 1) the particles interact only through the electric fields; 2) the environment of each particle is isotropic or at least has cubic symmetry.

7.1.1. *f*-sum rule

The cross section σ_{ab} satisfies a very important sum rule due to Thomas, Reiche and Kuhn called the *f*-sum rule,

$$\frac{m_e c}{2\pi^2 e^2 \hbar} \int_0^\infty \sigma_{ab} dE = N_e. \quad (7.5)$$

As before, N_e is the number of electrons in the particle. I will also define the dipole strength function $S(\omega)$ as

$$S(\omega) = \frac{2m_e \omega}{\pi \hbar e^2} \text{Im} \alpha(\omega). \quad (7.6)$$

The strength function has units of oscillator strength per unit energy, and satisfies the sum rule $\int_0^\infty S d\omega = N_e$. It is common to express energy-integrated cross sections in units of the sum rule for a single electron. This is the quantity “*f*” in the sum rule’s name. For any physical excitation, the absorption cross section is finite over some spectral region $\Delta\omega$. The *oscillator strength* f_i associated with the excitation may then be defined

$$\int_{\Delta\omega} d\hbar\omega S(\omega) = f.$$

The theoretical strength for a discrete excitation a is given by the formula

$$f_a = \frac{2m}{\hbar^2} | \langle 0 | x | a \rangle |^2 \hbar\omega_i.$$

There are many derivations of the *f*-sum rule. One derivation starts from the operator relation $[x, [H, x]] = 1/2m_e$. Another derivation that is easily applied to the TDDFT follows from the short-time behavior in an external dipole field, $V(t) =$

$e\mathcal{E}_0\delta(t)$. The ground state wave function Ψ_0 is perturbed by the field; to linear order the perturbed wave function is

$$\Psi(t=0_+) = \Psi_0 + \frac{e\mathcal{E}_0}{i} \sum_j \Psi_a \langle \Psi_a | x | \Psi_0 \rangle.$$

Each eigenstate Ψ_a evolves in time with the phase factor $\exp(-iE_a t)$. Again to linear order in the perturbation, the dipole moment is given by

$$e\langle x \rangle = -ie^2\mathcal{E}_0 \sum_a (e^{-i\omega_a t} - e^{i\omega_a t}) \langle \Psi_a | x | \Psi_0 \rangle^2, \quad \text{where } \omega_a = E_a - E_0.$$

Taking the derivative with respect to time, we find the time rate of change of the dipole moment at $t=0_+$ as

$$e \frac{d\langle x \rangle}{dt} \Big|_{0_+} = 2e^2\mathcal{E}_0 \sum_a \omega_a \langle \Psi_a | x | \Psi_0 \rangle^2,$$

On the other hand, we can evaluate this derivative using the equation of continuity. Immediately after the external field is applied, the particle current is given by $\langle \vec{j}(r) \rangle_{0_+} = e\hat{x}\mathcal{E}_0 n(r)/m$. Then

$$e \frac{d\langle x \rangle}{dt} \Big|_{0_+} = \int d^3r x \nabla \cdot \langle \vec{j}(r) \rangle_{0_+} = e\mathcal{E}_0/m \int d^3r x \frac{dn(r)}{dx} = e\mathcal{E}_0 N_e/m$$

Comparing the last two equations gives back the sum rule in the form

$$\sum_a \omega_a \langle \Psi_a | x | \Psi_0 \rangle^2 = \frac{N_e}{2m}.$$

This shows the close connection between the sum rule and the short-time behavior of the system.

The first application of TDDFT was to describe the photoionization of atoms.³⁶ The theory has since been widely applied to clusters, molecules, and bulk matter. My own research is on applications of the TDDFT, starting with the collective excitations of atomic clusters but going on to other electronic systems and other properties. Most of the effort was in the numerical aspects of solving the equations. My work in this area was in collaboration with K. Yabana. For reference, our published work on TDDFT is in Refs. 17-43. We started using a method developed in nuclear physics, and this proved to be quite useful. In the next section I will briefly describe the leading algorithms, their advantages and disadvantages.

7.2. Methods to solve the TDDFT equations

There are many mathematical formulations of the TDDFT. Most of them assume that the solution is close to the ground state wave function, so that the time-dependent equation can be linearized. In this section we will distinguish ground state orbitals with a superscript (0), for example $\phi_i^0(\mathbf{r})$ for the i -th orbital. The TDDFT satisfies an important condition, that the ground state remain stable under the time evolution. It is easy to see for this case that the time-dependent orbitals evolve only

by a overall phase factor, $\phi_i(\mathbf{r}, t) = e^{-i\epsilon_i t} \phi_i^0(\mathbf{r})$ with ϵ_i the Kohn-Sham eigenvalue. Let us now consider a small deviation $\delta\phi_i(\mathbf{r}, t)$ from this solution, expanding the time-dependent wave function as

$$\phi_i(\mathbf{r}, t) = e^{-i\epsilon_i t} (\phi_i^0(\mathbf{r}) + \delta\phi_i(\mathbf{r}, t)).$$

Putting the above wave function into Eq. (7.2) we have

$$H_{KS}[n_0 + \delta n + \dots] (\phi_i^0(\mathbf{r}) + \delta\phi_i(\mathbf{r}, t)) = \epsilon_i \phi_i^0 + \epsilon_i \delta\phi_i + i \frac{\partial}{\partial t} \delta\phi_i.$$

The transition density δn may be obtained by a first-order expansion of $n = \sum_i |\phi_i|^2$,

$$\delta n = \sum_i (\phi_i^* \delta\phi_i + \delta\phi_i^* \phi_i).$$

Next collect all the first order terms to obtain

$$(H_{KS}^0 - \epsilon_i) \delta\phi_i + \phi_i^0 \frac{\delta H_{KS}}{\delta n} \delta n = i \frac{d\delta\phi_i}{dt}$$

Here the Kohn-Sham operator H_{KS}^0 is defined $H_{KS} = H_{KS}[n_0]$. The functional derivative of H_{KS} with respect to n contains two terms, one from the direct Coulomb field and one from the exchange-correlation potential. The LDA functional derivative has the form

$$\frac{\delta H_{KS}(\mathbf{r})}{\delta n(\mathbf{r}')} = \frac{e^2}{|\mathbf{r} - \mathbf{r}'|} + \frac{dV_{xc}}{dn} \delta^3(\mathbf{r} - \mathbf{r}').$$

In the literature, $\frac{\delta H_{KS}}{\delta n}$ is often denoted by $K(\mathbf{r}, \mathbf{r}')$ and in fact the identification $K = \frac{\delta H_{KS}}{\delta n}$ is called the adiabatic approximation. Once the equations are linearized, the time dependence may be found by Fourier transforming with the integral $\int dt e^{i\omega t}$ and solving for each frequency separately. Let us write the perturbed wave function for frequency ω as $\delta\phi_i(\mathbf{r}, t) = \phi_i^+(\mathbf{r}) e^{-i\omega t} + \phi_i^-(\mathbf{r}) e^{i\omega t}$. It is necessary to consider both positive and negative frequencies because δn involves both ϕ and its complex conjugate. The resulting equations of motion are then

$$(H_{KS}^0 - \epsilon_i) \phi_i^\pm + \frac{\delta H_{KS}}{\delta n} \delta n \phi_i^0 = \pm \omega \phi_i^\pm. \quad (7.7)$$

The transition density δn in this equation is given by $\delta n = \sum_i (\phi_i^0 \phi_i^+ + \phi_i^0 \phi_i^{-*})$. Eqs. (7.7) form a generalized eigenvalue problem; in general the equations have a nontrivial solution only for particular values of ω .

Several choices can be made at this point to represent ϕ_i^\pm and solve the equations. One way to proceed is to expand the unknown functions ϕ_i^\pm in eigenstates of H_{KS}^0 ,

$$\phi_i^+ = \sum_c X_{ci} \phi_c^0$$

$$\phi_i^- = \sum_c Y_{ci} \phi_c^0$$

It turns out that it is only necessary to include the unoccupied orbitals in summing over c . Eq. 7.7 can then be expressed as the matrix eigenvalue problem

$$\begin{pmatrix} A & B \\ -B & -A \end{pmatrix} \begin{pmatrix} X \\ Y \end{pmatrix} = \omega \begin{pmatrix} X \\ Y \end{pmatrix} \quad (7.8)$$

The matrix elements A , B , are given by

$$A_{ci,c',i'} = \delta_{c,c'}\delta_{i,i'}(\epsilon_c - \epsilon_i) + \int d^3r d^3r' \psi_c^*(\mathbf{r})\psi_i(\mathbf{r}) \frac{\delta H_{KS}(\mathbf{r})}{\delta n(\mathbf{r}')} \psi_{i'}^*(\mathbf{r}')\psi_{c'}(\mathbf{r}')$$

$$B_{ci,c',i'} = \int d^3r d^3r' \psi_c^*(\mathbf{r})\psi_i(\mathbf{r}) \frac{\delta H_{KS}(\mathbf{r})}{\delta n(\mathbf{r}')} \psi_{i'}^*(\mathbf{r}')\psi_{c'}(\mathbf{r}')$$

The dimensionality of the matrix is the number of particle-hole combinations in the space. The normalization of the eigenvectors (X, Y) is a tricky point. The matrix in Eq. (7.8) is not Hermitian, so it requires a biorthogonal basis to expand the matrix in eigenvectors. The conjugate vector to the eigenvector (X, Y) is the eigenvector of the conjugate equation, which is easily seen to be $(X^*, -Y^*)$. The orthogonality and normalization conditions then become

$$\sum_{ci,c'i'} (X_{c'i'}^* X_{ci} - Y_{c'i'}^* Y_{ci}) = \delta_{ci,c'i'} \quad (7.9)$$

Another approach to solving Eq. (7.7) is to include an external field and solve the resulting inhomogeneous equations. Taking the field of the form $U(r)(e^{-i\omega t} + e^{i\omega t})$ the equations are

$$(H_{KS}^0 - (\epsilon_i \pm \omega))\phi_i^\pm + \frac{\delta H_{KS}}{\delta n} \delta n \phi_i^\pm = U \phi_i^0 \quad (7.10)$$

The direct solution of these equations is called the Sternheimer method. It can be done efficiently using the conjugate gradient algorithm, if the operator on the left-hand side has a sparse matrix representation. It can also be convenient to solve them with the help of the Green's function for the operator H_{KS} , as is done in the linear response method described below.

7.2.1. Linear response formula

Here we seek an equation for the transition density, δn . As a first step, we formally solve eqs. (7.10) for ϕ_i^\pm ,

$$\phi_i^\pm = \frac{1}{(H_{KS}^0 - \epsilon_i \pm \omega)} (U + \delta n \frac{\delta H_{KS}}{\delta n}) \phi_i^0$$

Next we insert this in the expression for the transition density, to obtain

$$\delta n = \sum_i \phi_i^0 \left(\sum_{\pm} \frac{1}{H_{KS}^0 - \epsilon_i \pm \omega} \right) \phi_i^0 \left(U + \frac{\delta H_{KS}}{\delta n} \delta n \right)$$

To make the equation more concrete, let us put in explicitly the coordinate dependence. The sum over the wave functions with the single-electron Green's function will be denoted $\chi_0(r, r')$,

$$\chi_0(r, r') = \sum_i \phi_i^0(r) \left(\sum_{\pm} \frac{1}{H_{KS}^0 - \epsilon_i \pm \omega} \right)_{r, r'} \phi_i^0(r')$$

Then the equation has the appearance

$$\delta n(r) = \int d^3 r' \chi_0(r, r') \left(U(r') + \int d^3 r'' \frac{\delta H_{KS}}{\delta n} \delta n(r'') \right)$$

The formal solution of the equation is

$$\delta n = (1 - \chi_0 \frac{\delta H_{KS}}{\delta n})^{-1} \chi_0 U \quad (7.11)$$

It can be solved by representing the operator $(1 - \chi_0 \frac{\delta H_{KS}}{\delta n})$ as a matrix in coordinate space or in reciprocal space. The matrix is then inverted directly or by some iterative method.

7.3. Dynamic polarizability

We now describe how to compute the dynamic polarizability using the different methods to solve the TDDFT equations.

The linear response method is very easy to apply. One takes the external field of the dipole form, $U(r) = e\mathcal{E}_0 x$, calculates the response δn , and finds the resulting dipole moment:

$$\alpha_{xx}(\omega) = \frac{D}{\mathcal{E}_0} = \frac{e^2}{\mathcal{E}_0} \int \delta n(r) x d^3 r$$

Because the response is linear, the field strength \mathcal{E}_0 can be taken with any convenient value.

The dynamic polarizability can also be calculated from the direct solution of Eq. (7.2). One starts with the ground state, and perturbs the system with an impulsive external field, $U(r, t) = -kx\delta(t)$. The orbitals acquire a phase factor due to the perturbation. Immediately following they are given by

$$\phi_i(t = 0_+) = e^{ikx} \phi_i^0$$

These are taken as the initial conditions for the time-dependent equations. Solving the equations to evolve the wave functions forward in time, one can construct the time-dependent density, $n(t)$. A time-dependent polarizability can be defined as the ratio of the dipole moment to the strength the perturbing field,

$$\alpha_{xx}(t) = \frac{e^2}{k} \int d^3 r x n(t).$$

The dynamic polarizability is then given simply by the Fourier transform,

$$\alpha(\omega) = \int_0^\infty e^{-i\omega t} \alpha(t)$$

Note that all frequencies are obtained in one calculation of the time evolution. This makes this method quite efficient if the polarizability is needed over a large range of frequencies.

If one use the matrix eigenvalue method, the dynamic polarizability is given by Eq. (7.3) summing over the eigenmodes a and taking the excitation energies as the eigenfrequencies ω_a . The necessary dipole matrix elements $\langle 0|x|a \rangle$ are given by

$$\langle 0|x|a \rangle = \sum_{ij} \langle i|x|j \rangle (X_{ij}^a + Y_{ij}^a) \quad (7.12)$$

In principle, this method requires that all the eigenvalues and eigenvectors be found, which is certainly a disadvantage if only a limited frequency range is of interest.

7.4. Dielectric function

The methods described above can all be applied to infinite periodic systems, with some modifications. A very popular technique is to use a plane-wave basis, since it is convenient for expanding the periodic Bloch wave functions. I will show here an alternative method we developed that uses the coordinate space representation to solve the real-time equations.⁴² It is easy to impose the periodic boundary conditions of the Bloch wave functions on the computed orbitals in a cubic unit cell. However, there are two subtleties. First, one cannot take the usual form for the dipole field, $V(r) = \mathcal{E}_0 x$, because it differs from cell to cell, and anyway gets large at large r . The other problem is that the currents can induce a surface charge on the dielectric. This charge is crucial to provide the restoring force for a plasmon at zero momentum, for example. Both these difficulties can be overcome by using a gauge field. We divide the electric field into a periodic part that can be represented with an ordinary potential V , and a uniform electric field arising from the gauge field $\hat{x}A(t)$:

$$\vec{\mathcal{E}} = -\vec{\nabla}V - \hat{z} \frac{dA}{dt}.$$

The equations of motion are derived from the Lagrangian of a unit cell Ω : we derive the dynamic equations from the Lagrangian:

$$L = \int_{\Omega} d^3r \left(\frac{\sum_i |\vec{\nabla} \phi_i / i - eA \hat{z} \phi_i|^2}{2m} - \frac{1}{8\pi} \vec{\nabla}V(r) \cdot \vec{\nabla}V(r) + en(r)V(r) + en_{ion}(r)V(r) + V_{xc}[n(r)] + V_{ion}[\rho(r, r')] \right) - \frac{\Omega}{8\pi} \left(\frac{dA}{dt} \right)^2 - i \int_{\Omega} d^3r \sum_i \phi_i^* \frac{\partial \phi_i}{\partial t}. \quad (7.13)$$

Here the ϕ_i are the Bloch wave functions of the electrons, normalized so that $n(r) = \sum_i |\phi_i(r)|^2$ is the electron density. The volume of the unit cell is Ω . In these formal equations, we use units with $\hbar = c = 1$.

The other pieces of the first integral are the usual terms in the Kohn-Sham energy functional. The term $en(r)V(r)$ gives the direct Coulomb interaction of the

electrons, except for the surface charging. The ionic interaction is separated into a long-range part that can be associated with an ionic charge density $n_{ion}(r)$ and a short-range part V_{ion} . The latter depends on the orbital angular momentum of the electrons in typical *ab initio* pseudopotentials. It therefore depends on the full one-electron density matrix $\rho(r, r') = \sum_i \phi_i^*(r)\phi_i(r')$. We have emphasized this point because nonlocal interactions do not respect gauge invariance. The invariance is of course restored when the density matrix is gauged. Finally, the V_{xc} is the usual exchange-correlation energy density of density functional theory.

Requiring the Lagrangian action to be stationary gives equations of motion for ϕ_i and A and the Poisson equation for V . The variation with respect to ϕ_i^* gives the Kohn-Sham equations, and varying with respect to A gives its equation of motion:

$$\frac{\Omega}{4\pi} \frac{d^2 A}{dt^2} - \frac{e}{m} \sum_i \langle \phi_i | \nabla_z / i | \phi_i \rangle + \frac{e^2}{m} A N_e + \frac{\delta}{\delta A} \int_{\Omega} V_{ion} d^3 r = 0 \quad (7.14)$$

where $N_e = \int_{\Omega} d^3 r n(r)$ is the number of electrons per unit cell. The reason I have given so much detail is that we didn't arrive at the correct equations immediately. We first guessed at the form of the equations, and tried to solve them numerically. The solutions did not conserve energy, and we only found the correct equations after we had formulated the problem with the variational principle, Eq. (7.13). The lesson is that variational principles are very useful!

Let us now see how the gauge field treatment works in a simple analytically solvable model, namely the electron gas. As mentioned before, when the field A_0 is applied, there is no immediate response to the operator ∇ , since the wave function does not change instantaneously. However, in the Fermi gas, the single-particle states are eigenstates of momentum so the response remains $\langle \nabla \rangle = 0$ for all time. Putting this in Eq. (7.14), and dropping the pseudopotential term, the equation for A becomes simple harmonic motion, with the solution

$$A(t) = A_0 \cos \omega_{pl} t \quad (7.15)$$

where ω_{pl} is the plasmon frequency,

$$\omega_{pl}^2 = \frac{4\pi e^2 N_e}{m\Omega} = \frac{4\pi e^2 n}{m}. \quad (7.16)$$

One sees that the derivation here is much simpler than the usual one using the Coulomb gauge. There one formulates the response in a particle-hole representation, and takes the external field to be of the form $e^{iq \cdot r}$ with q finite. The dielectric function is then found by taking the $q \rightarrow 0$ limit.

8. TDDFT: numerical aspects

I discussed above the equations for the various methods to calculate the TDDFT, but there are also important numerical aspects that one needs to understand in order to apply the theory to large systems. In this section I will describe the computational issues for the configurational matrix method, the linear response method, and the real-time method.

8.1. Configuration matrix method

Eq. (7.8) is a nonhermitian matrix eigenvalue problem. It may be converted to Hermitian form as follows. The two equations are added and subtracted to give

$$(A + B)(X + Y) = \omega(X - Y)$$

$$(A - B)(X - Y) = \omega(X + Y)$$

Then eliminate $X + Y$ between the two equations to get

$$(A + B)(A - B)(X - Y) = \omega^2(X - Y)$$

The matrix $A - B$ is diagonal in the configuration representation with matrix elements $(A - B)_{ij,ij} = \epsilon_i - \epsilon_j$. Thus one can easily take the square root of $A - B$ and transform the last equation to

$$(A - B)^{1/2}(A + B)(A - B)^{1/2}W = \omega^2W \quad (8.1)$$

with

$$W = (A - B)^{1/2}(X - Y)$$

Once one has W , the vectors X and Y may be obtained by the formulas $X + Y = (A - B)^{1/2}W/\omega$ and $X - Y = (A + B)(A - B)^{1/2}W/\omega^2$.

If only a few configurations are important in an excitation, this method is an obvious choice. The case of a single configuration is especially simple. There are two energies that enter, the particle-hole excitation energy $\Delta\epsilon = \epsilon_c - \epsilon_i$, and the interaction matrix element $v = \int d^3r d^3r' |\phi_i(r)\phi_c^*(r')|^2 \delta H_{KS}(r)/\delta n(r')$. Putting this in eq. 8.1, one finds

$$\omega^2 = \Delta\epsilon(\Delta\epsilon + 2v)$$

and the amplitudes X, Y are found to be

$$X = \sqrt{\frac{\Delta\epsilon}{\omega}} \frac{v}{\Delta\epsilon - \omega} \quad Y = \sqrt{\frac{\Delta\epsilon}{\omega}} \frac{v}{\Delta\epsilon + \omega}.$$

If one calculates the oscillator strength with eqs. (7.3,7.12), one finds that it is independent of v . The interaction v changes the excitation energy, but also changes the dipole matrix element in a way that preserves f .

The configurational matrix method is widely applied, generally with a judicious truncation of the configurational space. Besides in the many quantum chemistry programs that use this method, it is also applied in condensed matter physics using either the momentum- or the coordinate-space representation⁴⁷ to calculate the matrix elements. However the configurational matrix method requires truncation of the particle-hole space to be practical for large systems. Without truncation, the dimension D of the matrices is $D = N_c N_e$. The direct solution of the eigenvalue problem requires of the order of D^3 arithmetic operations, thus giving an N^6 scaling

with system size. However, iterative methods may still be useful. Two popular iterative methods are the Lanczos method and the Davidson method. These are both Krylov space methods in the terminology of computational physics. One utilizes a space of vectors generated by applying the Hamiltonian operator to some initial vector. The Lanczos method is very straightforward, just diagonalizing the Hamiltonian matrix in this space. Unfortunately, it does not work very well when there are many states at high excitation. The Davidson method uses preconditioning of the Hamiltonian matrix to suppress the overemphasis on configurations with large diagonal energies in the Krylov space. It is often used in quantum chemistry programs. All of the iterative methods are slow if one is seeking highly excited states. Namely, the iterative methods work by extracting the eigensolutions one at a time, starting from an end of the spectrum. The iterative process for each state requires orthogonalizing to the solutions already extracted. This becomes time consuming when there are many states.

With truncation of the particle-hole space, the most time-consuming task is usually the calculation of the matrix elements. This requires of the order of $N_c^2 N_e^2 N_\phi$ operations. Storage of the matrix requires a memory of size $N_c^2 N_e^2$ which can also be a limitation. These scaling factor are listed in Table 7, comparing the numerical requirements of the different methods of the computer can also be limiting.

Table 7. Size scaling of various algorithms for TDLDA—general comparison: floating point operations (FPO) and memory requirements.

Method	FPO	Memory
Configuration matrix	$N_c^2 N_e^2 N_r$	$(N_c N_e)^2$
k -space response	$5M_\omega (N_k)^3$	N_k^3
Response (Sternheimer)	$M_\omega M_{it} M_H N_e N_r$	$N_R (N_e + N_c)$
Real-time	$N_e N_r M_H M_T$	$N_r (N_e + 4.5)$

8.2. Linear response method

The linear response method works directly in the vector space representing the orbitals. For example, in a momentum space representation, the matrix χ_0 has a dimension of N_k . This representation has been very commonly used in the last decade for calculating the dielectric properties of bulk solids. There are two computational demanding tasks to evaluate eq. (7.11). The first is to evaluate the matrix elements in ξ , which is done using the formula

$$\xi_0(\mathbf{k}, \mathbf{k}', \omega) = \sum_{ic} \sum_{\pm} \frac{\langle i | e^{i\mathbf{k}\cdot\mathbf{r}} | c \rangle \langle c | e^{i\mathbf{k}'\cdot\mathbf{r}} | i \rangle}{\omega - \epsilon_c \pm \epsilon_i + i\eta}$$

This requires $N_k^2 N_e N_c$ operations and would be the most demanding part of the computation if the space of unoccupied orbitals is unrestricted. Even with a restricted set of orbitals, one still has the matrix multiplication and inversion costs,

both of which are of order N_k^3 . This is clearly an improvement over the configuration method when one uses a complete space and direct diagonalization. In Table scaling, we have listed the computational costs assuming that the configuration space truncation is severe enough so that the matrix operations and storage are limiting. The factor M_ω is the number of frequencies one wishes to calculate.

8.3. Sternheimer method

Here one solves eq. 7.10 using the real-space representation so that sparse methods can be applied. Typically one uses the conjugate gradient method to solve the equations. The N -scalings are shown in Table 7. Unlike the previously discussed methods, storage is not limiting. However, the iteration process may be problematic; it is difficult to estimate the number of iterations M_{it} to get a converged solution. If the frequency is well away from the eigenmodes of the system, convergence may be possible with several hundred iterations. Close to the eigenfrequencies the method does not converge at all.

8.4. Real time method

In the real time method, the linear response is computed by applying an impulsive (δ -function in time) external potential to the electronic ground state, then calculating the expectation of some observable of interest as a function of time, and then Fourier transforming to get the frequency response. The real-time method is intrinsically of order $N_e N_\phi$, unlike other methods which are higher order in N unless the bases are truncated in some way. The N -scalings are shown as the last line in Table scaling. Like the Sternheimer method, the real-time method does not require huge memory resources. Note also that all frequencies are contained in the initial perturbation and thus the entire frequency response comes out of a single time-dependent calculation. This reminds one of the modern experimental techniques in spectroscopy, which are to measure a signal in time and then Fourier transform to get a frequency or a mass spectrum. However, the time integration is done stepwise and requires a large number of steps M_T . I analyze this below in describing some specific algorithms to do the time integration.

We begin with the analysis of a time-independent Hamiltonian H . Given a state ϕ_i^0 at time zero, the time evolution is expressed by the formula

$$\phi(t) = e^{-iHt} \phi_i^0 \quad (8.2)$$

The wave function is needed as a function of time with some interval Δt . Thus one computes for successive time steps as

$$\phi(t + \Delta t) = e^{-i\Delta t H} \phi(t).$$

If one allows oneself M operations applying H to a wave function, the best approximation one can make is to expand the above exponential in a M -order Taylor series. But if you tried this with desired values of Δt , you would not get a useful result. The

problem is numerical, that any arithmetic operation introduces a truncation error. Now let us decompose the error vector into the eigenstates of H , calling the highest eigenvalue $|H|$. The first arithmetic operation introduces a spurious component of the highest eigenvalue, and each successive step in the expansion of the exponential multiplies that component by $\Delta t|H|/n$. For the desired Δt this is typically much larger than one, and the spurious component is dominant after some steps. Even using a small time step, it is important to carry out an expansion of the exponential to some higher order. This method was first used in a nuclear physics context,⁴⁸ and it was found that the 4th order expansion is especially useful. This is connected with an important requirement for the numerical representation of the exponential operator, that there not be any eigenvalues with modulus greater than one. Otherwise the vector would blow up under repeated application of the operator. To analyze the series expansion method, let us denote the N -order expansion by e_N , $e_N^{ix} = \sum_n^N \frac{(ix)^n}{n!}$. It is easy to see that e_1 is unsuitable:

$$|e_1^{i\Delta t|H|}|^2 = 1 + (\Delta t|H|)^2 > 1$$

On the other hand, the fourth-order expansion has the norm

$$|e_{(4)}^{ix}|^2 = 1 - \frac{8x^6}{4!^2} + \frac{x^8}{4!^2}. \quad (8.3)$$

This is less than one if $x = \Delta t|H| < \sqrt{8}$. In practice, the states of interest have small values of x and the decrease of norm for states of large x do not affect the observables. This method is the one we applied in most of our publications and is used in the code `real_time_dft.f` provided in our package of programs.

There is actually a better method, called the leapfrog, which can easily be derived from a discretized version of the variational principle, eq. (7.1). We take as variational variables the wave functions at discrete time steps, $\phi_n = \phi(r, n\Delta t)$, and approximate the time derivative as $(\phi_{n+1} - \phi_n)/i\Delta t$. The variational functional eq. (7.1) becomes

$$\Delta t \sum_n E_{KS}[\phi_n] - \sum_n \phi_n^* (\phi_{n+1} - \phi_n)/i.$$

Taking the variation with respect to ϕ_n^* yields the set of equations

$$\phi_{n+1} = \phi_{n-1} + 2i\Delta t H \phi_n. \quad (8.4)$$

Like the previous method, there is a limit on how large one can choose Δt . To derive the limit, first note that eq. 8.4 is invariant under the transformation $t \rightarrow t \pm n\Delta t$. Thus the time translations form a group, and the eigenstates have the time dependence $e^{i\lambda n\Delta t}$ for some value of λ that depends on the eigenstate. Substituting this form in Eq. 8.4, we arrive at the following relation,

$$\phi_{n+1} = e^{i\lambda\Delta t} \phi_n = \phi_n e^{-i\lambda\Delta t} + 2i\epsilon\Delta t \phi_n. \quad (8.5)$$

Solving for ϵ in terms of λ leads to

$$\sin(\lambda\Delta t) = \epsilon\Delta t. \quad (8.6)$$

from which it is clear that if $|\epsilon\Delta t| > 1$ the equation cannot be satisfied for λ real. An imaginary part to λ leads to an exponential growth that causes the algorithm to break down. Therefore we arrive at the condition $|H|\Delta t < 1$ for use of the leapfrog method. An example of this method in use is Ref. 49. It should be noted that it requires more care on initialization because it uses information from the previous two time steps. An error in the initialization makes an oscillation with period $2\Delta t$ and amplitude approximately equal to the magnitude of the error. However, this oscillation does not grow over time.

Besides norm conservation, the algorithm needs to conserve energy very accurately to be useful. In principle the TDDFT equations do conserve energy, but that is not guaranteed numerically. In practice, both the above algorithms produce acceptable energy conservation if Δt is small enough to conserve the norm.

We can now easily analyze the number of time steps M_T in Table 7. Let's suppose we want to get the spectrum with a resolution of Γ on the line width. To get this resolution in the Fourier transform of the real-time response, the time interval T must satisfy^d $T > 2\pi\hbar/\Gamma$. On the other hand, from the above discussion we learned that the time step must satisfy $\Delta t < \hbar/|H_{KS}|$. In the real-space method, the highest eigenvalues are determined by the mesh spacing, $|H_{KS}| \approx 6/(m(\Delta x)^2)$. Putting this together for a typical case ($\Delta x = 0.3 \text{ \AA}$, $\Gamma = 0.1 \text{ eV}$), we find $M_T = 30,000$.

9. Applications of TDDFT

The main application of the linearized TDDFT is to optical and electric properties such as photon absorption cross sections, polarizabilities, and dielectric functions. I will only give a sample of the many kinds of systems that the method can be applied to, discussing metal clusters, various carbon systems, and two condensed materials.

9.1. Simple metal clusters

I shall show the results of numerical calculations of the TDDFT on excitations in clusters of alkali metals and of silver. These elements have a single valence electron in an *s*-shell, giving them a relatively simple electronic structure. It is always helpful to have simple models to compare with, and for these systems a simple qualitatively understanding is possible with the surface plasmon model. Here one assumes that the electrons behave classically and are free within the system, and compute the dynamics generated by the direct Coulomb field. This problem can be solved exactly for spherical systems. The frequency of the surface plasmon excitation is given by

$$\omega_{sp}^2 = \frac{4\pi e^2 n}{3m}, \quad (9.1)$$

^dThis is the full width at half maximum when the Fourier transform is filtered with the function $1 - 3(t/T)^2 + 2(t/T)^3$.

where n is the density of conduction electrons^e. Because all the valence electrons move coherently in the model, the predicted oscillator strength f is equal to the number of atoms in the metal particle. A more sophisticated model is the jellium model, which has the quantum mechanics of the electron wave functions, but replaces the ionic potentials of the real materials by a uniform positively charge background. Table 8 shows a sample of the predicted excitation energy of the strong transitions and comparison to experiment.

These metal clusters do show a highly collective transition, confirming the existence of the surface plasmon mode. However, its frequency is lower than the surface plasmon formula predicts. For example, for sodium clusters the formula gives $\omega_{sp} \approx 3.4$ eV but the observed surface plasmon is lower by about 20% for clusters in the size range of several tens to hundreds of atoms. One possibility to explain the red shift would be with a lower density of atoms in the cluster than in the bulk, but that is not supported by DFT calculations of the cluster structure. Another mechanism to explain the red shift is the spillover of the electrons, a quantum effect that the orbitals extend farther than the boundaries of the background charge distribution. This mechanism can be analyzed quantitatively by calculating the TDDFT response in the jellium model. There is a computer code, called JellyRpa, that I wrote and distributed⁵⁰ to calculate the response of spherical jellium, making no other approximations on the dynamics.

Indeed there is an effect of the spillover. The peak is red shifted from the surface plasmon formula by 10%, about half of what is needed to explain the empirical position. Another possibility is that the local density approximation might not be accurate enough. In particular, we will see shortly that the local approximation to exchange can produce serious errors in infinite systems. This question was addressed in finite clusters by Madjet *et al.*,⁵² who examined and compared the different treatments of exchange. They found that the LDA exchange was quite satisfactory for sodium clusters, and could not be the reason for the discrepancy.

Lastly, the jellium approximation might be inadequate; the full TDDFT of course includes a realistic treatment of the ionic potentials. Using pseudopotentials for the sodium ions, one obtains somewhat different results depending on the prescription used for the pseudopotential. The simplest realistic prescription gives very similar results to the jellium model. However, another prescription,⁵³ produces an additional red shift, bringing the surface plasmon close to the observed position. In the end, it is rather disquieting that a seemingly small change in the ionic potential would have a very noticeable effect on the absorption spectrum.

Lithium clusters show an even larger red shift than sodium: the surface plasmon formula predicts 4.6 eV, while the observed peak in the absorption spectrum is lower by 35%.⁵⁴ From the Table, one sees that the TDDFT reproduces the observed position with its shift quite well. Here it is much easier to understand how the shift arises from the ionic potential. The ionic potential is different for s and p waves

^eIn applying this formula, we will use the value of the density of atoms in the bulk solid.

because there is a core s orbital that is excluded from the valence wave function but no corresponding excluded p state. Thus, the ionic potential is effectively more attractive for p orbitals. This makes it easier to excite the electrons from the ground state, and lowers the excited state energies. The experimental peak is rather broader than in sodium and has an asymmetric shape. These features are also reproduced by the TDDFT.¹⁷

Table 8. Surface plasmon in simple metal clusters

Element	Cluster size	Surface Plasmon	TDDFT	Exp.
Na	8	3.4 eV	2.7 eV	2.5 eV ⁵¹
Li	139	4.6	2.9 ¹⁷	2.9
Ag	8	5.4	3.2,3.9 ⁴⁰	3.2,3.9

There is also a large red shift of the surface plasmon for silver clusters. Here the formula gives 5.4 eV, but the observed peak in the absorption much lower, closer to 3.5 eV. For the Ag₈ clusters, shown in Table 8, the excitation is split into two peaks. Both are reproduced in the TDDFT assuming a certain geometry for the cluster (see Ref. 40 for details). The origin of the red shift is not the same as in the lithium. Silver has a filled d shell just below the valence s shell which is rather easy to polarize, effectively screening the charge of the valence electrons. This physics is contained in the TDDFT, provided the d electrons are treated explicitly. One can even separate out their influence in doing the calculation. Effectively, the charges are screened by a factor of two.

I finally want to mention the strength of the surface plasmon. In sodium clusters, the strength is close to the theoretical maximum of f equal to the number of s electrons. In lithium, there is some reduction that can be motivated by putting an effective mass $m^* > m$ into the surface plasmon formula. In silver, the theoretical reduction factor is 1/4 corresponding to the effective charge screening, $e^* = e/2$. However, while theory and experiment are in accord for sodium and lithium, the experimental reduction of strength for silver is not as large as predicted. Probably one should wait for additional experiments before drawing a conclusion here.

9.2. Carbon structures

There is a rich variety of conjugated carbon systems, ranging from small clusters and molecules to fullerenes, nanotubes, and graphite. I use the word *conjugated* to mean that the orbitals can be classified as π -type or σ -type and that the π orbitals are at the Fermi surface^f. A very simple theory, the Hückel model, provides the same kind of guidance for these systems as the jellium model does for the alkali metal clusters. The π orbitals on different atoms couple rather weakly, and the

^fThe classification requires also that the carbons lie on a plane or a surface that can be considered locally planar. The σ and π orbitals have even or odd reflection symmetry, respectively.

Hückel models the wave function by the amplitude of the π orbital on each carbon, constructing the eigenstates from the simple hopping Hamiltonian $H = -\beta \sum_{ij} c_i^\dagger c_j$. Here the sum i, j runs over pairs of adjacent carbon atoms. The hopping parameter β depends on distance d between carbon atoms when that varies; see Ref. 41 for a parameterization.

Table 9. $\pi - \pi$ transitions in conjugated carbon systems

System	Number of carbons	Hückel model	TDDFT	Exp.
chain	9	1.7 eV	4.6 eV	4.2 eV
polyene	10	2.1	3.2	3.4
benzene	6	5.2	6.9	6.9
fullerene	60	2	3.4-6.6	3.8-6

A sampling of the results for strong transitions is shown in Table 9. The first entry is the carbon chain C_9 , taken from Ref. 37. The Hückel model predicts that the lowest particle-hole excitation is at 1.7 eV, and the number agrees well with the difference of the Kohn-Sham eigenvalues for the orbitals just above and below the Fermi energy. However, the time-varying potential in the equations of the TDDFT increase the frequency of the oscillation, pushing the state up to 4.6 eV. From the Table it may be seen that this is close to the observed position. The behavior is similar in the polyenes (molecules of structure $CH_2(CH)_nCH_2$): the particle-hole gap in the Kohn-Sham spectrum is well reproduced by the Hückel model, but the interaction pushes the collective excitation up in frequency. The energies for the polyene $C_{10}H_{12}$ are shown in the Table, taken from Ref. 41.

The optical response of benzene is very well known experimentally, making it a good test of the theory. Besides the numbers in the Table, Fig. 3 of the absorption experiment shows an excellent agreement between theory and experiment. The sharp peak at 6.9 eV is the strong π - π transition; its predicted strength $f = 1.1$ is only 25% off from the measured value. As one goes higher in energy, there are many more states that can be excited, and the real-time TDDFT gives a prediction for the entire spectrum. The broad bump centered at 18 eV is due to the more tightly bound σ electrons. Its center position and overall width is correctly described by the theory. Of course the TDDFT does not describe all the details of the spectrum. Between the two main peaks one can see some tiny structure in the experimental spectrum that reminds one of tuft of grass. These are the so-called Rydberg states, having a very loosely bound electron in the Coulomb field of the ion. These states cannot be described in the LDA because of its incorrect asymptotic potential field.

9.3. Diamond

I will take diamond as an example of the application of the TDDFT to a bulk insulator. Fig. 4 shows the imaginary part of its dielectric function. The strong absorption centered at 12 eV is fairly well reproduced, but the band gap, seen by the energy where the function becomes nonzero, is too low by a couple of eV.

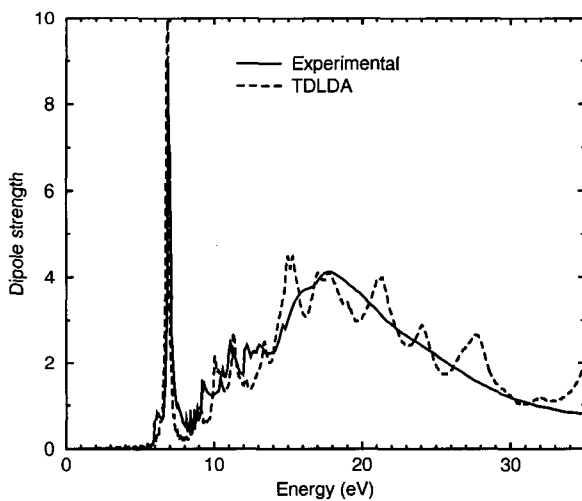


Fig. 3. Comparison of experimental and theoretical absorption spectrum in benzene, from Ref. 41.

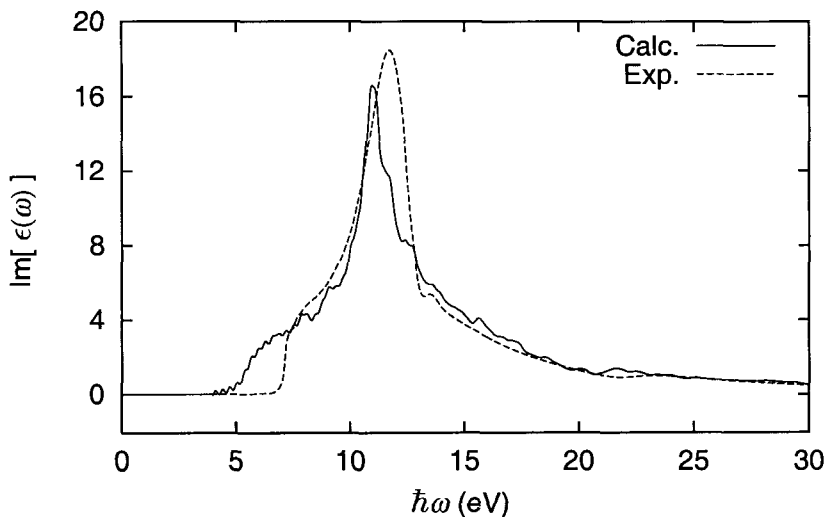


Fig. 4. Imaginary parts of the dielectric function $\epsilon(\omega)$ for diamond, calculated by TDDFT⁴⁵ and compared with experiment.⁵⁵

Nevertheless the error here is compensated elsewhere in some way: if one uses this result to calculate the dielectric constant (real part of the dielectric function at zero frequency), one finds excellent agreement with experiment. See Ref. 45 for further details.

9.4. Other applications

In this section we briefly mention three other applications of of TDDFT: electron-vibration coupling, optical rotatory power, and nonlinear excitation.

We have seen that the DFT works very well for vibrational properties, and the TDDFT is a useful theory for the excitations. What about the coupling between them? The best way to see if it applies to the couplings is to try it out. Fortunately this is very simple theory to treat the couplings called the reflection approximation. It requires the probability distribution of the nuclear coordinates (arising from zero point motion or thermal excitation or both), and the response is calculated by averaging over that distribution. This approximation can be derived by a semiclassical treatment of the coupling, using a short-time expansion of the response of the system.⁵⁶ This joins well to the TDDFT, which we saw could also be viewed as a short-time expansion. I won't go into the details here, but just show some of the results for benzene.⁴⁶ That molecule makes a good test case because essentially all of its properties are known. Besides the strong π - π transition at 6.9 eV that we saw earlier, there are π - π excitations at lower energy that are forbidden by symmetry to be excited by dipole photons. However, the zero-point vibrational motion breaks the symmetry and allows the states to be weakly excited. Table 10 shows the oscillator strength for the three excitation in the π - π manifold. The strength range over three orders of magnitude, and theory reproduces the numbers to 35% or so. This is really a remarkable achievement of the TDDFT.

Table 10. Oscillator strength of the excitations of benzene in the π - π manifold. See 46 for details.

$f/10^{-3}$	TDDFT	CASSCF	Exp.
$^1B_{2u}$	1.6	0.5	1.3
$^1B_{1u}$	59	75	90
$^1E_{1u}$	1100		900-950

Molecules or clusters that lack a center of symmetry will interact differently with left- and right-circularly polarized photons. In the language of multipoles, such molecules have a mixed parity and the electric dipole and magnetic dipole operators are coherent. The interference terms that are responsible for the optical rotatory power have the form

$$R_n = -\frac{e^2 \hbar}{2mc} \langle \Phi_0 | \sum_i \vec{r}_i | \Phi_n \rangle \cdot \langle \Phi_n | \sum_i \vec{r}_i \times \vec{\nabla} | \Phi_0 \rangle. \quad (9.2)$$

where the first matrix element is the ordinary electric dipole and the second is the magnetic dipole. This quantity can be extracted with the real-time response to an impulsive dipole field. The difference from what we did before is that the dipole moment that is measured as a function of time is not the electric but the magnetic. For details see our article, Ref. 39. We tried it on a simple ten-atom molecule and on the chiral fullerene C_{76} . We found that the theory give the correct order of magnitude of the chiral properties, but on a quantitative level was much less reliable than when calculating oscillator strengths. For the lowest transitions in the ten-atom molecular, the R_n values had the correct sign but were a factor of three off in magnitude. I should mention that the calculations were done with the LDA functionals, and it might be that the GGA could give quite different results.

All the previous applications have used the linear response of the system. The nonlinear response is described by hyperpolarizability coefficients,⁵⁷ extending the power series eq. (7.4) to second and higher terms in the electric field,

$$e\langle x \rangle = - \sum_j \alpha_{ij} \mathcal{E}_j + \frac{1}{2} \sum_{jk} \beta_{ijk} \mathcal{E}_k \mathcal{E}_j + \frac{1}{6} \sum_{jkl} \gamma_{ijkl} \mathcal{E}_k \mathcal{E}_j \mathcal{E}_l + \dots$$

The second-order nonlinear polarizability γ_{ijk} is only observable if the molecule can be oriented. It is important in technology for devices that can control optics by external electric fields. For a simple case, the water molecule, the TDDFT give a result that is about a factor of two different from the experimental. Unfortunately, the derived numbers depend on the choice of energy functional. There are also situations where the systems are exposed to extremely large fields. One of these is with excitation of clusters or molecules by slow-moving, highly charged ions. Such processes have been calculated in Ref. 58, 59. Another application of strong-field TDDFT is the excitation of clusters by intense laser fields. Calculations have also been made in this area,⁶⁰ but so far one has not made detailed enough calculations to model some of the most interesting experimental observations.

9.5. Limitations

In the diamond spectrum one saw that the theoretical excitations started at a lower energy than experiment. This is a generic problem of the TDDFT in infinite systems, that the band gap is too small. The band-gap problem originates in the LDA treatment of exchange. To see the origin of the problem, one needs only to look in more detail at the exchange contribution to the electron energies in the Fermi gas. The Fock energy of an electron of momentum k is given by

$$- \sum_i \langle ki | \frac{e^2}{|r - r'|} | ik \rangle = - \frac{e^2 k_F}{\pi} \left(1 + \frac{k_F^2 - k^2}{2kk_F} \log \left| \frac{k + k_F}{k_F - k} \right| \right). \quad (9.3)$$

From this equation one sees that the exchange potential of an electron in a Fermi gas has a weak logarithmic singularity at the Fermi surface. Particle-hole excitations across the Fermi surface have a higher energy for a given momentum difference

than the quadratic kinetic energy functional. Because the singularity is weak, it doesn't show up for small systems. Clearly, any local approximation will miss the singularity. An effective, but computationally costly method to overcome this is to calculate the electron energies from the many-body perturbation theory.⁶¹ In the GW approximation, the electron-self energy is calculated including exact exchange. The GW theory gives an enormous improvement to the band gap. But the computational demands of the theory has so far restricted its application to relatively simple systems.

The GW approximation fixes the energies of single-electron excitations, but the electron-hole interaction can also be important as well. In a large system with a band gap, the electron and hole are attracted to each other by their Coulomb interaction, and the bound states are called excitons. This part of the interaction is treated by a zero-range approximation in the density functional theory, so it has no possibility to produce weakly bound hydrogenic states. This is fixed up with an approved treatment of the exchange called the Bethe-Salpeter equation. This is even more computational intensive than the GW, but has achieved the best success so far in describing the optical properties in insulators near the band gap.

Acknowledgments

We would like to thank T. Fennel for help in preparing the lecture notes, J.-I. Iwata for preparing the computer programs and J. Giansiricusa for additional help on the distribution package. GB acknowledges discussions with C. Guet, J. Rehr, and E. Krotscheck. GB's research mentioned in these lectures was supported by the Department of Energy under Grant FG06-90ER-40561.

References

1. J. P. Perdew, K. Burke, and M. Ernzerhof, *Phys. Rev. Lett.* **77**, 3865 (1996).
2. J. P. Perdew, S. Kurth, A. Zupan, and P. Blaha, *Phys. Rev. Lett.* **82**, 2544 (1999).
3. M. Gell-Mann and K. A. Brueckner, *Phys. Rev.* **106**, 364 (1957).
4. E. Teller, *Rev. Mod. Phys.* **34**, 627 (1962).
5. D. M. Ceperley and B. J. Alder, *Phys. Rev. Lett.* **45**, 566 (1980).
6. J. P. Perdew and A. Zunger, *Phys. Rev. B* **23**, 5048 (1981)
7. U. Barth and L. Hedin, *J. Phys. C* **5**, 1629 (1972).
8. A. D. Becke, *Phys. Rev. A* **38**, 3098 (1988).
9. P. J. Stevens, *et al.*, *J. Phys. Chem.* **98**, 11623 (1994).
10. R. van Leeuwen and E. J. Baerends, *Phys. Rev. A* **49**, 2421 (1994).
11. N. Troullier and J. L. Martins, *Phys. Rev. B* **43**, 1993 (1991).
12. C. Hartwigsen, S. Goedecker, and J. Hutter, *Phys. Rev. B* **58** 3641 (1998).
13. A. Castro, A. Rubio and M. J. Stott, preprint arXiv:physics/0012024.
14. W. H. Press, *et al.*, *Numerical Recipes. The Art of Scientific Computing*, Second Edition, (Cambridge University Press, Cambridge, 1992), Sect. 19.6.
15. T. L. Beck, *Rev. Mod. Phys.* **72**, 1041 (2000).
16. J. Chelikowsky, *et al.*, *Phys. Rev.* **50** 11355 (1994).
17. K. Yabana and G. F. Bertsch, *Phys. Rev. B* **54**, 4484 (1996).
18. J.-L. Fattebert and J. Berholc, *Phys. Rev. B* **62**, 1713 (2000).

19. S. Goedecker, *Reviews of Modern Physics* **71**, 1085 (1999).
20. J. Kim, F. Mauri, and G. Galli, *Phys. Rev. B* **52**, 1640 (1995).
21. P. Ordejón, *Phys. Stat. Sol. B* **217**, 335 (2000).
22. S. Baroni and R. Resta, *Phys. Rev. B* **33**, 7017 (1986).
23. M. Hybertson and S. Louie, *Phys. Rev. B* **34**, 5390 (1986).
24. Asada and Tera, *Phys. Rev. B* **46**, 13599 (1992).
25. J. Cho and M. Scheffler, *Phys. Rev. B* **53**, 10685 (1996).
26. E. G. Moroni, *et al.*, *Phys. Rev. B* **56**, 15629 (1997).
27. C. Kohl and G. F. Bertsch, *Phys. Rev. B* **60**, 4205 (1999).
28. W. Krätschmer, *et al.*, *Nature* **347**, 354 (1990)
29. G. F. Bertsch, A. Smith, and K. Yabana, *Phys. Rev. B* **52**, 7876 (1995).
30. J. Kohanoff, *et al.*, *Phys. Rev. B* **46**, 4371 (1992).
31. A. M. Lee, N. C. Handy, and S. M. Colwell, *J. Chem. Phys.* **103**, 10095 (1995).
32. V. Anisimov, *et al.*, *Phys. Rev. B* **48**, 16929 (1993).
33. J. Bouchet, B. Siberchicot, F. Jollet, A. Pasturel, *J. Phys. Condensed Matter* **12**, 1723 (2000).
34. S. Savrasov, G. Kotliar, and E. Abrahams, *Nature*. **410**, 793 (2001).
35. P. Dirac, *Proc. Cambridge Phil. Soc.* **26**, 376 (1930).
36. A. Zangwill and P. Soven, *Phys. Rev. A* **21**, 1561 (1980).
37. K. Yabana and G. F. Bertsch, *Zeit. Phys. D* **42**, 219 (1997).
38. K. Yabana and G. F. Bertsch, *Phys. Rev. A* **58**, 2604 (1998).
39. K. Yabana and G. F. Bertsch, *Phys. Rev. A* **60**, 1271 (1999).
40. K. Yabana and G. F. Bertsch, *Phys. Rev. A* **60**, 3809 (1999).
41. K. Yabana and G. F. Bertsch, *Int. J. Quant. Chem.* **75**, 55 (1999).
42. G.F. Bertsch, J-I. Iwata, A. Rubio, and K. Yabana, *Phys. Rev. B* **62**, 7998 (2000)
43. J-I Iwata, K. Yabana and G. F. Bertsch, *J. Chem. Phys.* **115**, 8773 (2001).
44. K. Yabana, G. F. Bertsch, and A. Rubio, preprint arXiv: phys/0003090.
45. G. F. Bertsch, J. I. Iwata, A. Rubio, and K. Yabana, *Phys. Rev. B* **62**, 7998 (2000).
46. G. F. Bertsch, A. Schnell, and K. Yabana, *J. Chem. Phys.* **115**, 4051 (2001).
47. I. Vasiliev, S. Ogut, and J. Chelikowsky, *Phys. Rev. Lett.* **82**, 1919 (1999).
48. H. Flocard, S. Koonin, and M. Weiss, *Phys. Rev. C* **17**, 1682 (1978).
49. J. J. Rehr and R. Alben, *Phys. Rev. B* **16**, 2400 (1977).
50. G. Bertsch, *Comp. Phys. Comm.* **60**, 247 (1990). The program JELLYRPA may be downloaded from the author's Web site, www.phys.washington.edu/bertsch.
51. K. Selby, *et al.*, *Phys. Rev. B* **43**, 4565 (1991).
52. M. Madjet, C. Guet and W. R. Johnson, *Phys. Rev. A* **51**, 1327 (1995).
53. S. G. Louie, S. Froyen, and M. L. Cohen, *Phys. Rev. B* **26**, 1738 (1982).
54. C. Brechignac, *et al.*, *Phys. Rev. Lett.* **70**, 2036 (1993).
55. *CRC Handbook of Chemistry and Physics* (CRC Press, Boca Raton, 77th ed. 1996). p. 12-133.
56. E. Heller, *J. Chem Phys.* **68**, 2066 (1978).
57. P. N. Butcher and D. Cotter, *Elements of Nonlinear Optics*, (Cambridge University Press, Cambridge, 1990), eq. 4.83.
58. K. Yabana, T. Tazawa, P. Bozek, and Y. Abe, *Phys. Rev. A* **57**, R3165 (1998).
59. R. Nagano, K. Yabana, T. Tazawa, and Y. Abe, *Phys. Rev. A* **62**, 062721 (2000).
60. C. A. Ullrich, P. G. Reinhard, and E. Suraud, *J. Phys. B* **31**, 1871 (1998).
61. L. Hedin, *J. Phys. Condens. Matter* **11**, R489 (1999).

This page is intentionally left blank